Pan African University
Institute of Water and Energy Sciences

PAN-AFRICAN UNIVERSITY
INSTITUTE FOR WATER AND ENERGY SCIENCES
(Including CLIMATE CHANGE)

Master Dissertation

Submitted in partial fulfilment of the requirements for the Master degree in

Water engineering

Presented by

HAYKEL ALIMI

TITLE: Spatial and temporal variability of rainfall under an arid climate condition:

Case of Gafsa Basin, Southern Tunisia.

Defended on 15/11/2021 before the Following Committee:

Chair	Dr. Abdelhadi Ammari	University of Blida-Algeria
Supervisor	Prof. Habib Abida	University of SFAX-Tunisia
Co-supervisor	Dr.Jemai Hiba	University of SFAX-Tunisia
External Examiner	Dr. Raphael Muli Wambua	University of Kenya
Internal Examiner	Prof. Heddam Salim	University of Skikda-Algeria

Academic Year: 2019-2020

DECLARATION

I hereby declare that this thesis, submitted only to the Pan-African University; Institute of Water and Energy Sciences (Including climate change) PAUWES, entitled "Spatial and temporal variability of rainfall under an arid climate condition Case of GAFSA Basin Southern Tunisia" has been prepared by me under the guidance and supervision of
Pr. Habib ABIDA.

Signed  Date 09/10/2021

HAYKEL ALIMI

This thesis has been submitted for examination with our approval as the University supervisors.

Signature  Date 09/10/2021

Prof. HABIB ABIDA

DEDICATION

To my dear mother Hania

To my father Mabrouk

To my brothers Imed & Achref

To my sister Kawther

And all my friends.

I dedicate this work with all

The love and respect I have for them.

Haykel ALIMI

ACKNOWLEDGEMENT

Upon completion of this work, I give thanks to all those who have offered me their support, their advice and friendship.

My first sincere thanks and gratitude are forwarded to the Pan-African University PAUWES for the opportunity and the experience that I got during the two years.

Many thanks for my supervisor Professor HABIB ABIDA, for the support criticism and help given during the process. His unlimited encouragement and advice was for me invaluable support and helped to complete this work. I well appreciate the wealth of knowledge, rigor of thought and the great human and moral qualities he has.

Many thanks for Dr. Hiba Jemai, member of GEOMODELE Laboratory at the Faculty of Sciences of Sfax, for her help with the simulation methods, encouragement and support.

Special thanks to Dr. Achraf Melki, member of GEOMODELE Laboratory at the Faculty of Sciences of Sfax, for providing the data used this study.

My sincere thanks and gratitude go to Professor Chérifa Abdelbaki, coordinator of water program at the Pan-African University; Institute of Water and Energy Sciences (Including climate change) PAU-WES for the encouragement and desire to see me through.

Many thanks to the head and director of PAUWES, Dr. Abdellatif Zerga for the constant passion and desire to ensure all the academic and non-academic components of my stay at the PAUWES Institute were well taken care of, I thank him very much for his moral support.

To all the PAUWES and GIZ/DAAD staff .My gratitude to my fellow colleagues in PAUWES, for the encouragement, criticism and hunt for enlightenment during these two years. May the path stay true.

Lastly, to my Family and friends, my heart felt gratitude for standing by me during this period.

ABSTRACT

Understanding the rainfall variability should put into consideration several aspects in order to highlight facts and trying to recommend solutions. In a continental scale the Republic of Tunisia is one of the countries inside the MENA region and extremely affected by the global climate change condition same like all the countries abound. The study of the variability should identify the problem statements according to adequate and meaningful data sets to get into concrete results to cope with climatic challenges and cite recommendations therefore considered as a priority for future life. The basin of GAFSA located in the south western of the Tunisia republic, statistical analysis following several models based on rainfall data recorded during around 56 years from 1960 to 2015 at 18 rainfall stations highlighted that the GAFSA region is characterised by a significant variability in precipitation, this instability derived from a sequence of analysis in which both a descriptive and a spectral analysis (Wavelet analysis) combine to show up specific components reflects this spatial-temporal variability of precipitation such as , Altitude, longitude, latitude and the frequency of rainfall.

Résumé

La compréhension de la variabilité des précipitations doit prendre en compte plusieurs aspects afin de mettre en évidence les faits et d'essayer de recommander des solutions. A l'échelle continentale, la République tunisienne est l'un des pays de la région MENA et extrêmement affectée par les conditions du changement climatique global, comme tous les pays du voisinage. L'étude de la variabilité devrait identifier les problèmes selon des ensembles de données adéquats et complets afin d'obtenir des résultats concrets pour faire face aux défis climatiques et citer des recommandations considérées comme une priorité pour la vie future.Le bassin de GAFSA situé au sud-ouest de la république tunisienne, l'analyse statistique suivant plusieurs modèles basés sur les données pluviométriques enregistrées pendant environ 56 ans de 1960 à 2015 dans 18 stations pluviométriques a mis en évidence que la région de GAFSA est caractérisée par une variabilité significative des précipitations, cette instabilité dérivée d'une séquence d'analyse dans laquelle à la fois une analyse descriptive et une analyse spectrale (analyse en ondelettes) se combinent pour mettre en évidence des composantes spécifiques reflètent cette variabilité spatio-temporelle des précipitations telles que l'altitude, la longitude, la latitude et la fréquence des précipitations.

Table of Contents

DECLARATION....ii
DEDICATION....iii
ACKNOWLEDGEMENT....iv
ABSTRACT....v
Résumé....vi
Table of Contents....vii
List of Figures....x
List of Tables....xi
CHAPTER ONE....12
Introduction....12
Background information....12
Case study....13
Problem statement....13
Objectives....14
CHAPTER TWO....15
LITERATURE REVIEW....15
2.1. Review of water resources....15
2.2. The importance of water resources availability....15
2.3. Spatial and temporal variability of rainfall....16
2.4. Effects of the North Atlantic Oscillation (NAO)....16
2.5. Historical review of the global phenomena:....16
2.5.1. Historical Records of Niño events:....16
2.5.2. The North Atlantic Oscillation (NAO)....17
Description of the different indices:....18
Positive NAO index: (Fig.1)....18
Negative NAO index: (Fig.2)....19
2.6. Drought....20
2.7. Hydrological drought....21
2.8. Impacts of droughts....21
2.9. Rainfall regime in arid to semi-arid climates....22
CHAPTER THREE....23
MATERIALS AND METHODS....23
3.1. Presentation of the adopted procedure....23
3.2. Adopted Procedure and Methodology....23

3.3. Control of observation series 25
3.3.1. Independence test 25
3.3.2. Stationarity test 25
3.3.3. Homogeneity test 25
3.4. Analysis of annual data 25
3.4.1. Frequency classification (Principal Component Analysis) 25
3.4.2. Rainfall Index (RAI) Classification 26
3.4.3. Index of deviation from the mean (Em) 26
3.4.4. Detecting unexpected changes 27
3.4.5. Frequency distribution 27
3.5. Analysis at a monthly scale 28
3.5.1. Standardised Precipitation Index (SPI) 28
3.6. Software packages used 29
CHAPTER FOUR 31
STUDY AREA AND DATA BANK 31
4.1. PRESENTATION OF THE STUDY AREA 31
4.1.1. Geographical location 31
4.1.2. Geological setting 32
4.1.3. Reliefs 33
4.1.4. Soils 34
4.1.5. The plant cover 35
4.1.6. Hydrography 36
4.2. DATA BANK 38
4.2.1. Source of data 38
4.2.2. CLIMATIC CONTEXT OF THE STUDY AREA 39
CHAPTER FIVE 41
SPATIAL AND TEMPORAL STUDY OF RAINFALL VARIABILITY 41
5.1. Preliminary tests: 41
5.1.1. Independence test 41
5.1.2. Stationarity test 41
5.1.3. homogeneity test 42
5.2. Data fitting: 43
5.2.1. Introduction 43
5.2.2. Normal distribution 43
5.2.3. Log-Pearson Type 3 distribution 43
5.2.4. GEV Distribution 43

5.2.5. Goodness-of-fit test 44
5.2.6. Conclusion 47
5.3. Descriptive analysis 48
5.4. Subdivision of the Gafsa watershed: 54
5.4.1. Subdivision based on PCA 54
5.4.2. Subdivision based on the cumulative rainfall index 57
5.4.3. Spatial distribution of rainfall according to the principal component analysis (PCA) and the cumulative rainfall index 60
5.5. Spectral analysis 63
5.5.1. Continuous wavelet analysis 63
5.5.2. Identification of the main modes of rainfall variability 64
CHAPTER SIX 73
GENERAL CONCLUSIONS AND RECOMMENDATIONS 73
REFERENCES 75

List of Figures

Fig 1.NAO Positive phase 18
Fig 2.NAO Negative phase 19
Fig 3: Flow chart of the adopted methodology 24
Fig 4 Situation map of the GAFSA Basin (ATLAS, 2014) 32
Fig 5 Geological map of the Gafsa Basin (ATLAS, 2014) 33
Fig 6 Geomorphology of GAFSA region (ATLAS, 2014) 34
Fig 7 Soil map of GAFSA (ATLAS, 2014) 35
Fig 8 Land cover GAFSA region (ATLAS, 2014) 36
Fig 9 Hydrography of GAFSA Region (ATLAS, 2014) 37
Fig 10 Rainfall stations distribution in Gafsa Basin 38
Fig 11 Temperatures variation in GAFSA (ATLAS, 2014) 39
Fig 12 Monthly rainfall distribution (ATLAS, 2014) 40
Fig 13 Stationarity test 42
Fig 14 Normal distribution 45
Fig 15 Log-Pearson Type 3 distribution 45
Fig 16 GEV distribution 46
Fig 17 Variability of minimum and maximum rainfall 50
Fig 18 Distribution of the average annual rainfall in the GAFSA catchment area 50
Fig 19 Variation of average rainfall with latitude 52
Fig 20 Variation of average rainfall with altitude 53
Fig 21 Variation of average rainfall with longitude 53
Fig 22 Scatter plot of rainfall stations by PCA 55
Fig 23 Variation of average rainfall with altitude 56
Fig 24 Annual variation of the cumulative rainfall index in group 1 57
Fig 25 Annual variation of the cumulative rainfall index in group 2 58
Fig 26 Annual variation of the cumulative rainfall index in group 3 58
Fig 27 Annual variation of the cumulative rainfall index in group 4 59
Fig 28 Annual variation of the cumulative rainfall index in group 5 59
Fig 29 Annual variation of the cumulative rainfall index in group 6 60
Fig 30 Subdivision of the basin into homogeneous zones based on the cumulative rainfall index (Melki and Abida, 2014) 60
Fig 31 Local spectra of wavelet analysis of monthly rainfall (Group 1) 67
Fig 32 Local spectra of wavelet analysis of monthly rainfall (Group 2) 70
Fig 33 Local spectra of wavelet analysis of monthly rainfall for Group 2(cont.) 71
Fig 34 Local spectra of wavelet analysis of monthly rainfall for Group 3 72

List of Tables

TAB 1 Classification of drought according to frequency (Smith et al.,1993) . **Erreur ! Signet non défini.**
TAB 2 Standardized percentage of drought (Mckee et al., 1995) 29
TAB 3 Characteristics of rainfall stations and series (CRDA-Gafsa, 2015) 39
TAB 4 the Chi-squared Test 46
TAB 5 Statistical characteristics of rainfall in the study area 48
TAB 6 Total explained variance 54
TAB 7 Quality of representation 56

CHAPTER ONE

Introduction

Background information

Throughout history, human societies have been severely impacted by hydrological extremes (drought and flood events). The collapse of various ancient civilizations, for instance, was attributed to the occurrence of hydrological extremes (Munoz et al., 2015). Fatalities and economic losses caused by drought and flood events have dramatically increased in many regions of the world over the past decades (Di Baldassarre et al., 2010; Winsemius et al., 2015) and currently, more than 100 million people per year are affected by hydrological extremes (UN-ISDR, 2016).

The climate at a specific location is defined as the 'average' weather conditions considered over a period of years (Skinner and Porter, 1987). Climate deals only with the long term weather conditions. Hence, the year to year fluctuations are disregarded by smoothening observations. The main factors affecting climate are precipitation and temperature at the Earth's surface, both varying greatly from one region to another. Indeed, rainfall distribution determines to a large extent the climatic potential of a region for plant and crop growth (FAO, 1978). Rainfall indirectly affects soil loss of arable and natural land by its capability of maintaining a vegetative cover (Baldassarre *et al.*, 2017).

Due to a slow evolution in time, drought is a phenomenon whose consequences take a significant amount of time with respect to its inception in order to be perceived by the socioeconomic systems. Taking advantage of this feature, an effective mitigation of the most adverse drought impacts is possible, more than in the case of other extreme hydrological events such as floods, earthquakes, hurricanes, etc., provided a drought monitoring system, able to promptly warn the onset of a drought and to follow its evolution in space and time. is in operation (Di and Bonaccorso, 2007).

Approximately 85% of natural disasters are related to extreme meteorological events (Obasi, 1994). Drought is one of the most complicated and least understood natural hazards, affecting more people than any other hazards (Wilhite, 2000). It is a slowly developing phenomenon, only indirectly affecting our life. Although drought first appears as below-average rainfall within a normal part of climate, it can develop as an extreme climatic event

and turn into a hazardous phenomenon which can have a severe impact on communities and water dependent sectors (McKee et al., 1993). Precipitation is the primary factor controlling the formation and persistence of drought conditions. Other climatic factors such as temperature, wind, and relative humidity are often associated with it in many regions of the world and can significantly aggravate its severity. In recent years, due to the effect of climate change drought studies are getting special attention (Byun and Wilhite, 1999).

Unlike other natural disasters, drought events evolve slowly in time and their impacts generally span a long period of time. Such features do make possible a more effective drought mitigation of the most adverse effects, provided a timely monitoring of an incoming drought is available. Among the several proposed drought monitoring indices, the Standardized Precipitation Index (SPI) has found widespread application for describing and comparing droughts among different time periods and regions with different climatic conditions. However, limited efforts have been made to show the role of SPI in drought forecasting.

Case study

Tunisia is situated in the extreme North of the African continent. It is characterized by an arid climate and limited water resources over most of its area. Rainfall distribution is very irregular in time and space throughout the country, where only about 220 mm of precipitation falls annually. As a specific area of study, the Region of GAFSA is located south-west of TUNISIA, between the high steppes and the Sahara. Surrounded by five governorates in the centre of three economic regions, the Region of GAFSA represents a transition between the country of the grain and that of the dates and it involves one of the oldest cities of the country (Gafsa City).

Problem statement

The region of Gafsa has been suffering of water shortage for years because of limited resources (decrease of precipitation yield and aquifer recharge due to climate change and other environmental violations) and ever increasing demands

Objectives

Broad Objectives:

- Examine temporal rainfall distributions at annual, monthly and daily time scales.

Specific Objectives:

- Detect hydrological extremes (floods and droughts) over the period (1965-2015).
- Examine spatial rainfall distributions for several historic flood events that occurred in the study basin.
- Detect rainfall variability modes via spectral wavelet analysis.

CHAPTER TWO

LITERATURE REVIEW

2.1. Review of water resources

Water resources development and management in the Middle East and North Africa (MENA) region have been driven by the highly specific characteristics of climate, geography and the resource itself. Water issues touch all subdivisions of society and all economic sectors. Population growth, rapid urbanisation and industrialisation, the expansion of agriculture and tourism, and climate change all put water under increasing stress. Given this growing pressure, it is critical that this vital resource is properly managed. In some countries, floods are among the most damaging weather events to communities. As for drought, it is a phenomenon that occurs in many parts of the world, of varying magnitude and duration. Tunisia experienced the most severe droughts during the periods 1937/1938, 1947/1948, 1960/1961, 1987/1988 and 1993/1994, especially in the centre and south, which have been confronted by three major dry periods during the last century. One (1935-1947) was observed in the first half and the other two (1979-1988 and 1992-2001) in the second half of the twentieth century. This finding confirms that dry conditions became more repetitive from the second half of the last century (ELLOUZE, 2010). In Tunisia, we point out that measures are needed to improve the capacity to adapt to hydrological variability and extreme events (floods and droughts) to reduce significant social, economic and environmental vulnerabilities.

2.2. The importance of water resources availability

Water demand already exceeds supply in many parts of the world, and more and more areas are expected to experience this imbalance in the near future. Water is required for agricultural, industrial, household, recreational and environmental uses. Demand for water for agricultural, household, recreational and environmental uses is rapidly increasing due to continuously increasing population and growing awareness of environmental, health and recreational issues. In spite of the fact that national water policies of many countries place household and industrial water needs at a higher priority level over other uses, there

are issues that limit the water availability for these uses at the points of consumption, resulting in water stress conditions. Many changes taking place at a rapid pace over different spatial scales including global climatic change. Land use changes and environmental degradation, further aggravate this problem. At the same time, the cost of developing new sources or expanding existing ones is continuously increasing as the most accessible water resources have already been tapped (UNESCO, 2003),(Vairavamoorthy, Gorantiwar and Pathirana, 2008)

2.3. Spatial and temporal variability of rainfall

The study (Jemai *et al.*, 2018) comes to show off the interconnection/correlation between precipitation and climate indices, such as the North Atlantic Oscillation (NAO) by examining the trend of rainfall variability based on the general shape of the dimensionless standardized precipitation ratio curves to identify the inter-annual variability as well as the period of deficit and excess of rainfall. The obtained results are then analysed by the continuous wavelet method to identify the origins of the precipitation temporal variations (dry and wet season).

2.4. Effects of the North Atlantic Oscillation (NAO)

Previous research has identified the North Atlantic Oscillation (NAO) as one of the dominant atmospheric patterns on the temporal evolution of precipitation and temperature in the Mediterranean area. The NAO is seen to markedly affect snowpack variability and water resource availability in many mountainous areas (López-moreno *et al.*, 2011). The correlation between rainfall and the North Atlantic Oscillation is tested initially by using the analysis of the evolution of extreme years: wet and very humid and dry and very dry years.

2.5. Historical review of the global phenomena:

2.5.1. Historical Records of Niño events:

Generated in the tropical pacific. El Niño Southern Oscillation (ENSO) events create a far-reaching system of climate anomalies that operate on a range of time scales important to society. ENSO influences extreme weather events such as drought, flooding, bushfires and tropical cyclone characterized by low atmospheric pressure, high winds and heavy rain

across vast areas of the earth and affecting hundreds of millions of people in agriculturally important areas of Australasia. Africa and the Americas (Gergis and Fowler, 2009).

ENSO is a coupled cycle in the atmosphere-oceanic system (Bjerkness ,1966,1969). It is an irregular phenomenon that alternates between two phases. El Niño and la NINA, approximately every 2-7 years. Generally, El Niño (la NINA) Events cause a warming (cooling) in tropical pacific and Indian oceans that enhance rainfall in western-eastern pacific regions (Allan et al., 1996). El NINO and el NINA are popular terms for alternating cold and warm phases of ocean temperatures in the eastern and central Pacific Ocean of the coast of South America (Jr and Landsea, 1999).

The el NINO-southern oscillation (ENSO) system is commonly considered as the best example of ocean/atmosphere interaction and one of the most relevant manifestations of interannual variability in the global climate system although the ENSO phenomenon is primarily observed in the equatorial pacific ocean and the bordering land areas. it has been shown that it induces worldwide climatic anomalies (tele-connections) in tropical and extra-tropical areas(Ortlleb, 1993). Ortlleb (1993) argued that these characteristics and the fact that many impacts and consequences of the ENSO/EL NINO anomalies are catastrophic explain that the phenomenon has received a particular attention in major current research programs (Global change, research program on the world climate, tropical oceans-Global Atmosphere project. etc.).

2.5.2. The North Atlantic Oscillation (NAO)

North Atlantic Oscillation (NAO) is an irregular fluctuation/variation of atmospheric pressure over the North Atlantic Ocean that has a strong effect on winter weather in Europe, Greenland, North-eastern North America, North Africa and North Asia. The NAO can occur on a yearly basis, or the fluctuations can take place decades apart. It is an oscillation because changes in atmospheric pressure are essentially a back and forth switching between two modes: a positive mode in which a strong subtropical high pressure is located over the areas of islands in Central North Atlantic while a strong low pressure system is centred over Iceland, and a “negative mode”, in which weaker high and low pressure systems are found over the same locations.

Description of the different indices:

Positive NAO index: (Fig.1)

During winters when the NAO is in its positive mode, the presence of the strong high-pressure and strong low-pressure systems produces warmer, wetter conditions over Northern Europe and most of north-eastern North America. This occurs because the polar-front jet stream tends to be free of large undulations (Rossby waves), and the jet stream's westerly winds funnel storms over the Mid-Atlantic states, between the strong North Atlantic pressure cells, and over Northern Europe. Moreover, under the positive NAO mode, colder conditions prevail over parts of Quebec. Newfoundland and Labrador, and western Greenland, and additional sea ice develops in Hudson Bay, Baffin Bay, and off western Greenland. Meanwhile, the Mediterranean Region experiences cool dry winter weather.

During the spring following a winter dominated by the positive NAO, warm sea-surface temperatures occur along the eastern seaboard of the United States and Canada's Maritime Provinces. Such warm-water conditions are possibly brought on by the close approach of the Gulf Stream to the coast, which may reduce the influence of the cold westward-moving long shore current that flows along the southern coasts of Newfoundland and Nova Scotia.

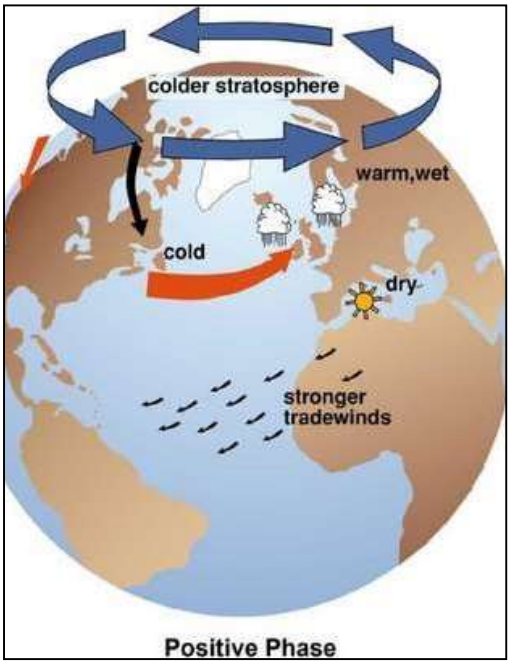

Fig 1.NAO Positive phase

Negative NAO index: (Fig.2)

During winters governed by the negative mode of the NAO, colder conditions are brought to eastern North America and Northern Europe mainly by more-frequent intrusions of Arctic air. North America receives additional snow, while Europe receives less precipitation than normal. The drier conditions over Northern Europe result from the weak state of the pressure cells over Iceland and the North Atlantic during the NAO's negative mode; the reduced pressure gradient over the region slows the pace of westerly winds, which allows cold, dry air to be drawn into northern Europe from Northern Russia and the Arctic. During such years a prominent northward-reaching arc in the polar-front jet stream, caused in part by blocking anticyclones that redirect the jet stream northward, allows warmer conditions to prevail from Hudson Bay to western Greenland. The reduced low pressure cell over Iceland, curves South across the North Atlantic to channel moisture and warm air to southern Europe.

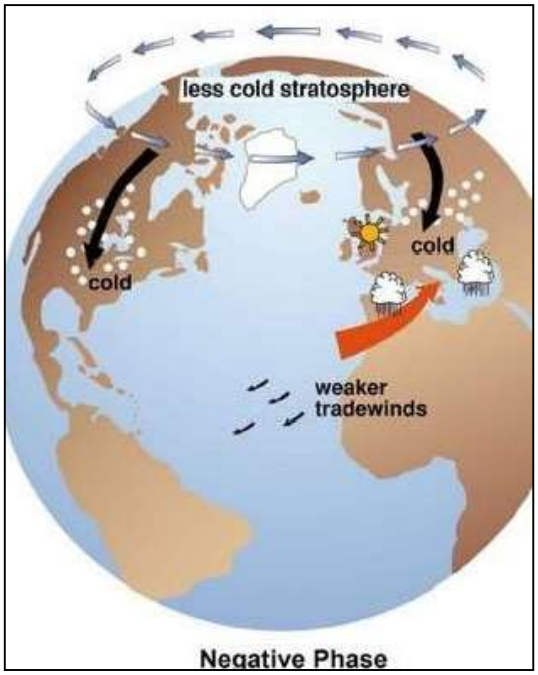

Fig 2.NAO Negative phase

During springs governed by negative NAO conditions, ocean-surface temperatures are colder off the eastern seaboard of the United States and Canada. In these years the warmer Gulf Stream follows a more southerly track, so the influence of the colder long shore current is stronger.

2.6. Drought

Drought is a leading cause of death worldwide. It accounts for 11% of natural disasters, and is the cause of almost half of the victims of natural disasters, affecting the economy and the environment (Obassi, 1994; Pruce, 1994; Wilhite, 2000). It causes crop losses (Austin et al., 1998; Leilah and Al-khateb, 2005), shortages and degradation of resources and desertification (Evans and Geerken, 2004) and even some fires (Pausas, 2004).

Drought should be considered as a relative rather than an absolute state. It occurs in areas with high and low rainfall, and in almost all climates. Scientists, policy-makers and the general public often associate it with arid, semi-arid or sub-humid regions, whereas in reality it occurs in most countries in both dry and humid regions. Drought is part of 6 climate, even if its extent and intensity vary on a seasonal or annual time scale. In many countries, including Australia, China, India and the United States of America, part of the country is affected by drought every year (The Notion, 2000). Thus, droughts are more frequent and severe in many countries of sub-Saharan Africa and have a devastating impact on their populations and economies (España, 2003). In view of the frequency of droughts and the magnitude of their effects, governments should attach greater importance to the development of a national strategy or policy to mitigate their economic, social and environmental consequences. An essential element of such a strategy is a monitoring system that provides early warning of the onset and end of drought, determines its intensity and makes this information available in a timely manner to a wide range of clients in many climate- and water-sensitive sectors, which in many cases should help to mitigate or avoid adverse impacts. Under some global change scenarios, the occurrence and impact of drought may increase in future years (Watson et al., 1997).

There is no universal definition of drought. It can be defined as a prolonged period of insufficient rainfall during one or more seasons that cause water deficits in some sectors of a country's economy (Khaldi, 2005). Drought is also defined in terms of the different areas

that interact with its effects. Therefore drought can be defined from a meteorological, hydrological point of view, agricultural or socio-economic (Wilhite and Glantz, 1985; Mokssit. El Khatri, 1996 and NDMC, 2005).

Drought is a recurring phenomenon of the climate. It is a temporary situation characterised by a lack of rainfall compared to normal values. It differs from other climatic fluctuations in that it sets in slowly and develops over months or even years. It can affect fairly large areas. However, its characteristics vary from one region to another. Nevertheless, drought should not be confused with aridity. Aridity, on the other hand, is a climatic characteristic of a given area; it is the permanent situation of low annual or seasonal rainfall (Lain, 2005).

Drought, which begins as a climatic event, gradually extends to all areas where water is involved. There are generally four types of drought: meteorological, agricultural, hydrological and socio-economic, to which a fifth type can be added: forest drought. These droughts may not always occur in the same area, demonstrate at the same time. However, dry weather remains the driving force behind the others.

2.7. Hydrological drought

Hydrological drought affects rivers and continental water bodies (ponds, lakes etc.) whose level or flow shows a lower value than that usually measured at the same time. Rivers and bodies of water may dry out temporarily partially or completely depending on the intensity and duration of the drought. Thus, drought occurs as a result of the prolonged weakening of rainfall inputs at the catchment level. A flow deficit systematically results within the watercourses. Groundwater recharge is reduced and irrigation operations are compromised (Mokssit, 1996).

2.8. Impacts of droughts

Drought is one of the most complex natural disasters. Its onset, end and severity are often difficult to predict. As with other disasters, the impacts of drought affect different sectors, economic, social and environmental (Khaldi A, 2005). Furthermore, drought is a dangerous natural phenomenon that affects areas with high rainfall as well as areas with low rainfall. Drought has various impacts. It affects our lives by putting pressure on water supply by

degrading the environment and human health through poor water quality, intensifying soil erosion and degrading the economy through reduced agricultural production capacity.

2.9. Rainfall regime in arid to semi-arid climates

Water resources are considered to be the most important elements in the arid regions where rainfall is low and evapotranspiration is high (Tweed et al., 2011). Precipitation in arid environments is often of the convective type: short duration, high intensity and spatial heterogeneity characterise them. A large majority (64%) of events in a semi-arid environment lasts less than or equal to an hour, in temperate climates, the frequency of this type of event is only 47%. The events of 7 hours or more are much more frequent in temperate environments (frequency of 13%) than in semi-arid environments (frequency of 3%). The brevity of the events characterises the rainfall regime of the semi-arid environment (Güntner, 2002).

CHAPTER THREE

MATERIALS AND METHODS

3.1. Presentation of the adopted procedure

An overall analysis of the system under study is established at different levels. First, we considered an analysis of the simplest configuration of the model on a large time scale (annual), and then we considered a gradual increase in complexity with a temporal decrease (from annual to monthly steps). This work is based on the downward approach to analyse the spatial-temporal variations of precipitation in Gafsa Basin at the annual and monthly time steps. The approach requires a complete and detailed study of precipitation at different time steps.

Following the analysis of the data series and the verification of certain statistical criteria, a delineation of the study watershed is established. Rainfall stations are classified into zones having climatic and physiographic similarities. These zones are delimited based on geographical boundaries. Then, for each time scale, a statistical analysis of drought characterization is started in each of the delimited areas. Next, we were interested in determining the recurrence and periodicity of rainfall variability and establishing estimates of probabilities, which may be useful in planning water resources management strategies.

3.2. Adopted Procedure and Methodology

The approach followed represents a complete and detailed study of rainfall at different temporal stages. Three time steps are taken into consideration, when studying the spatial-temporal variation of rainfall. For each time scale, a detailed analysis of the data series using different indices and statistical tools is established. The results obtained are then refined and adjusted by the analysis of the next step. The procedure adopted is summarised in Figure 3.

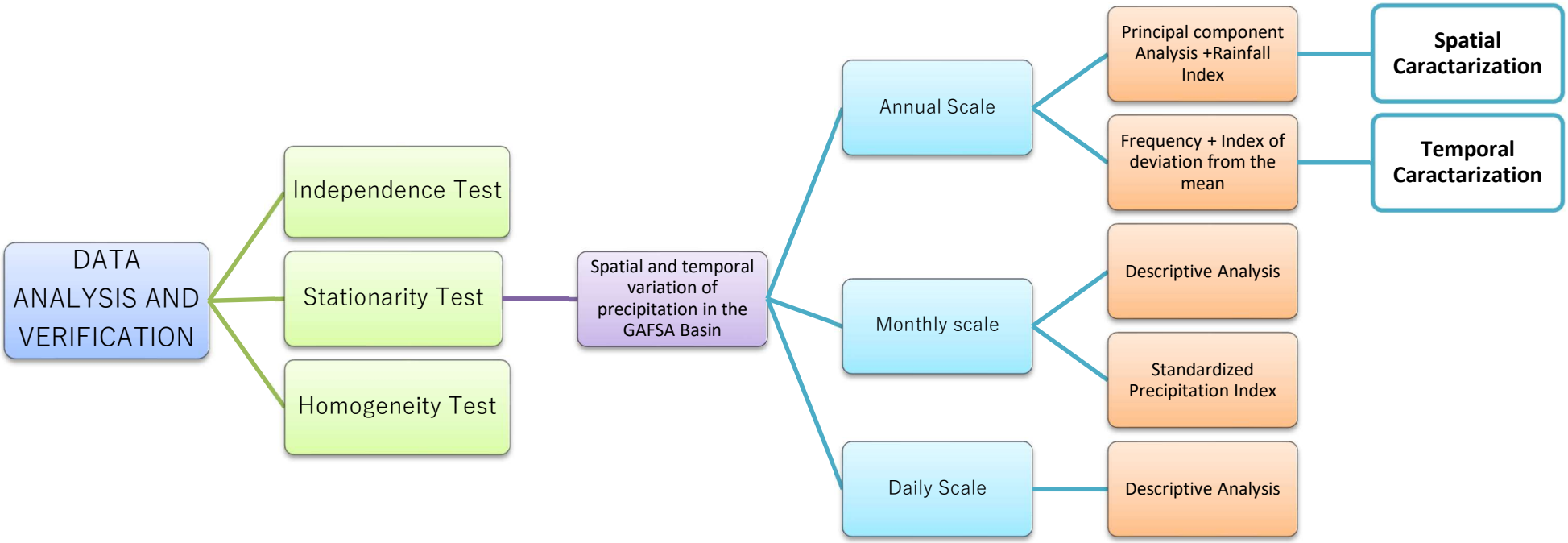

Fig 3: Flow chart of the adopted methodology

3.3. Control of observation series

Hydrological observations must verify certain statistical criteria, namely tests of independence, stationarity and homogeneity. Indeed, the series of observations must be independent, random, homogeneous and without tendency. These hypotheses have been verified using the HYFRAN-PLUS software (Hydro-Québec/NSERC, 1998).

3.3.1. Independence test

This is a test to verify that the probability of occurrence of an observation in a sample is not affected by any other observation in the same sample. A data series is temporally independent if no observation in the series has an influence on the observation that follows it. Data dependency varies according to the interval between successive items in a series. Indeed, independence can be measured by the significance of correlation between N-1(N sample size) pairs of the i^{th} and $(i+1)^{th}$ observation. If the correlation coefficient tends towards zero, the data series is assumed to be independent.

3.3.2. Stationarity test

This test is applicable in order to verify that the characteristics of the data set are invariant over time. The test is also called a trend test. The correlation coefficient of the Spearman test is used to check the trend of the series.

3.3.3. Homogeneity test

A sample is said to be homogeneous when all its observations come from the same statistical population. The homogeneity test is carried out using the Mann-Whitney test. The latter depends on the size of the samples and their corresponding ranks.

3.4. Analysis of annual data

3.4.1. Frequency classification (Principal Component Analysis)

Principal Component Analysis: A set of methods for performing linear transformations of a large number of variables which are cross-correlated to obtain a relatively small number of uncorrelated components. This approach facilitates the analysis by grouping the data into

smaller sets and eliminates problems of multi-collinearity between variables. Principal component analysis is similar to factor analysis, but it is an independent technique that is often used as a first step in factor analysis (Vogt, 1993). In the same context, Principal Component Analysis (PCA) and quality of representation are used to determine the dominant factors in the rainfall distribution across the study area. The objective of PCA is to graphically represent the relationships between annual precipitation series and at the same time to visualise the factors explaining their variability.

3.4.2. Rainfall Index (RAI) Classification

The rainfall index (RAI) is by definition the ratio of the annual rainfall to the average annual rainfall.

$$\mathbf{I_p = \frac{Pi}{Pm}\ (3.1)}$$

A year is considered wet if this ratio is higher than 1 and dry if it is lower than 1. To situate a rainfall in a long series of rainfall records, we use the deviation proportional to the average (Ipm) which differs from the rainfall index by subtracting 1 from this index.

$$\mathbf{I_{pm} = I_p - 1\ (3.2)}$$

The accumulation of indices from successive years makes it possible to identify the major trends, disregarding the slight fluctuations from one year to the next. When the sum of the indices increases, it is a wet trend. The trend is of the "dry" type; otherwise it is a "dry" trend. The study of similarity between the I_{pm} curves allows the definition of regions with identical characteristics. The results obtained by the Principal Component Analysis (PCA) and the I_{pm} rainfall index are used to re-establish the boundaries of the physiographic regions.

3.4.3. Index of deviation from the mean (Em)

The deviation from the average is the difference between the annual precipitation height (Pi) and the average annual precipitation height (Pm).

$$\mathbf{E_m = P_i - P_m\ \ (3.3)}$$

The deviation is positive for wet years and negative for dry years. A deficit year is defined as a year with less than average rainfall and a surplus year as a year with more than average rainfall. This index is commonly used to estimate the rainfall deficit at the year scale. The deviation from the median is the one most used by agro-meteorologists. Obviously, when the data sample is asymmetric, the difference between the mean and the median is large. Thus, this index makes it possible to visualise and determine the number of deficit years and their successions.

3.4.4. Detecting unexpected changes

First, we are interested in detecting changes in the annual averages of the precipitation series. Indeed, a break can be defined by a change in the probability law of the time series at a given moment, most often unknown (Lubès et al., 1998). Two statistical methods for detecting a break were used in this study: Pettitt's test (1979) and Hubert and Carbonnel's (1994) procedure for segmenting time series, These methods were applied using the KhronoStat Software developed by the (Maison des Sciences de l'Eau MSE) in Montpellier (Lubès et al., 1994).

3.4.5. Frequency distribution

The annual rains are classified in ascending order according to their probability of not being exceeded and then divided into five classes (Table 1)

Table 3.1 Classification of drought according to frequency (Smith et al.,1993)

F : Frequency or probability of non-exceedance	Category
F < 0.15	Very dry
0.15=<F < 0.35	Dry
0.35=<F < 0.65	Normal
0.65=<F < 0.85	Wet
F >=0.85	Very wet

The deviation from the mean and the rainfall index simply tell us which years are dry and which years are wet, as well as the general trends, the frequency analysis allows us to distinguish among the dry years those that are the most in deficit.

3.5. Analysis at a monthly scale

In order to refine the results of the annual rainfall analysis, we will move on to a monthly scale. The analysis is only interested in the already identified dry sequences with high annual variability. However, it does reveal the onset of droughts and determines their frequency and intensity.

3.5.1. Standardised Precipitation Index (SPI)

The SPI (Standardised Precipitation Index) is a statistical index of the probabilistic type. It was developed by the University of Colorado in the early 1990s (McKee, 1993). (Hayes et al., 1999) identified a number of advantages in favour of the use of the SPI:

- ✓ It is based only on rainfall and the calculations involved are quick and simple;
- ✓ SPI is flexible, as the time scale can be easily adapted to the type of assessment;
- ✓ The corresponding results are spatially consistent with the characteristics of the normal distribution on which it is based.

SPI also has some disadvantages. The choice of the distribution used to model the data is fundamental. For this purpose, the Gamma Distribution is generally accepted as it generally fits well with precipitation data. However, this is not always the case in arid and semi-arid regions (Ntale and Gan, 2003). Another delicate point concerns calibration. A sufficiently long and high quality series is required to make the distribution fit and thus calibrate the SPI. (McKee et al., 1993) and (Guttman, 1999) recommend that at least 30 years of quality data need to be available.

SPI has many advantages, most notably much greater flexibility, significantly simpler calculations, and results that are easily comparable in space and time. In addition, it is more transparent and better preserves the dimensionality of the data (Keyantash and Dracup, 2002). Moreover, according to Keyantash and Dracup (2002), SPI is currently the most effective tool for the analysis of meteorological drought. This index is deployed in order to characterize the drought at monthly intervals during a given period. It takes into account the previous humidity conditions. This index is calculated especially when rainfall is not normally distributed, especially for periods of less than 12 months. The reliability of the results obtained is mainly related to the length of the rainfall series. That is to say, the longer the size of the series, the better

and more reliable the results are. The calculation of this index makes it possible to establish the severity of the drought according to different classes (Table 2).

TAB 3.2 Standardized percentage of drought (Mckee et al., 1995)

Value of SPI	Interpretation
> 2	Extremely wet
1.5 - 1.99	Severely wet
1 - 1.49	Moderately wet
(-0.99) - 0.99	Close to normal
(-1) - (-1.99)	Moderately dry
(-1.5) - (-1.99)	Severely dry
< -2	Extremely dry

McKee et al (1993) used the SPI classification system in Table 2 to define drought intensity revealed by the rainfall analysis using the SPI. The same authors also defined the criteria for establishing, for any time scale, whether we are in the presence of a true drought period, which occurs when SPI is continuously negative and reaches the value of -1.0 (or lower). The drought period ends when the SPI value becomes positive. Any drought has a duration determined by the start and the end, an intensity determined by the monthly SPI values. The sum of the absolute (negative) SPI values represents the "change" in drought.

The values of the Standardised Precipitation Index (SPI) are calculated for three different time scales: short (3 months), medium (12 months) and long (24 months). For each climatic region the frequency, duration and intensity of drought at each time scale was determined.

3.6. Software packages used

In this work, many software packages are used such as Excel, Hyfran, ArcGIS and R software. These software packages are presented below.

- HYFRAN: The HYFRAN software allows a large number of statistical distributions to be fitted to a series of data that verify the assumptions of independence, homogeneity and stationarity. Thus this program allows to classify the data according to the frequency index ;

- SPSS (Statistical Package for the Social Sciences): developed by the International Business Machines (IBM). It is a data analysis and processing software. Its diversified functions make it possible to develop several types of analysis, such as principal component analysis, mainly used by scientists which help them process critical data in simple steps. Working on data is a complex and time consuming process, but this software can easily handle and operate information with the help of some techniques, in addition to it, the output can be obtained through graphical representation so that a user can easily understand the result.
- ArcGIS: this is a system developed by the American company Esri which allows the collection, organisation, management, analysis. communication and dissemination of geographical information;
- R software: R is a language and environment for statistical computing and graphics, R provides a wide variety of statistical (linear and nonlinear modelling, classical statistical tests, time-series analysis, classification, clustering. etc.) and graphical techniques, and is highly extensible.

CHAPTER FOUR

STUDY AREA AND DATA BANK

Introduction

This chapter consists of two complementary parts. The first is devoted to the presentation of the physical context of the catchment under study, including geology and relief, slopes, soil conditions, land use, stream network, groundwater in addition to climatic data, such as bioclimatic stages, temperature, evapotranspiration, wind and precipitation. In the second part of the chapter, data series used, their sources and characteristics are presented.

4.1. PRESENTATION OF THE STUDY AREA

4.1.1. Geographical location

Gafsa Basin, with a surface area of 7584Km^2, is located in the west of the southern territory of Tunisia between latitudes 34°05' to 34°45' and longitudes 8°03' to 9°35'. The basin is surrounded by 5 governorates: the governorate of Kébili in the south, Tozeur in the south west, Gabes in the south-east, Sidi Bouzid in the north-east and Kasserine in the north (Figure 4). At the continental scale, this region is located in the southern sector of the Saharan Atlas, corresponding to the transition zone between the Arab Maghreb countries and the African countries. It is limited to the north by the Atlas continuity of North Africa (Tunisian Atlas), to the south by the Saharan Platform, to the east by the western part of the Mediterranean and to the west by the Algerian Border.

The North Gafsa Aquifer System lies to the north of the Gafsa basin and extends almost over the entire North Gafsa catchment area. It occupies a surface 1572Km^2. This aquifer is bordered by the areas of OUM EL ARAIES and the governorate of KASSERINE to the north-west, while their north-eastern part is bordered by the mountain ranges of SIDI AICH and SNED. The northern and southern limits are the mountain of SIDI AICH and EL KSAR respectively.

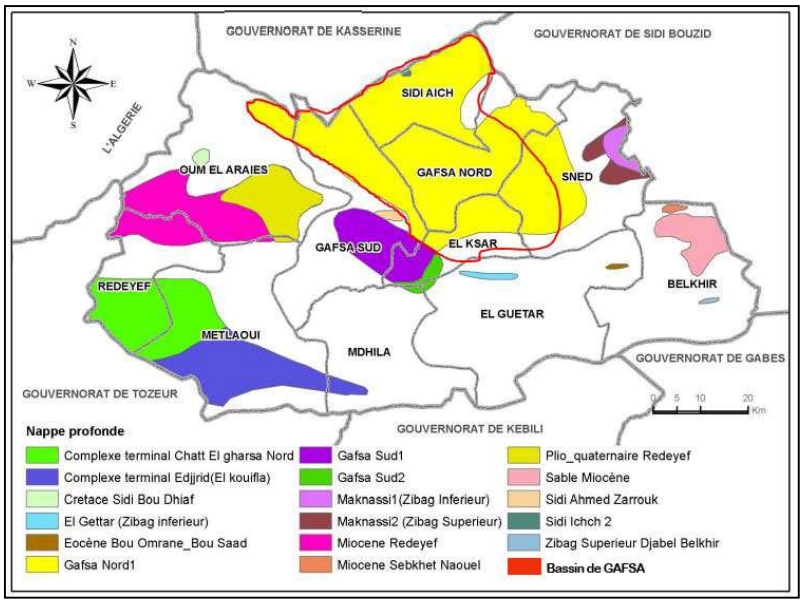

Fig 4 Situation map of the GAFSA Basin (ATLAS, 2014)

4.1.2. Geological setting

Figure 5 shows the geology of the entire Gafsa Basin. The Lower Cretaceous corresponds to the oldest series. These strata only outcrop in very small places in the centre and in the north-east of the basin. The outcrops of the Upper Cretaceous (Cenomanian and Turonian) occur in less extensive areas in the centre and north-east of the studied territory. The palaeogenic series are placed in sectors reduced to the western part of the basin. A remarkable development of the Neogene series (Miocene and Pliocene) over the whole of the region studied is distinguished. As for the Quaternary formations, they are the most dominant over the whole of the basin studied.

For the North Gafsa catchment area, (figure 5) expresses a large development of Quaternary deposits over the whole surface. The outcrops of the Mio-Pliocene can be seen mainly in the southern border areas and in a few regions to the north and south-west of the catchment area. The Upper Cretaceous occurs in very small areas to the south and north-east. As for the Lower Cretaceous formations, these are the oldest emerged series. These deposits only outcrop in one region northern border of a very limited extension.

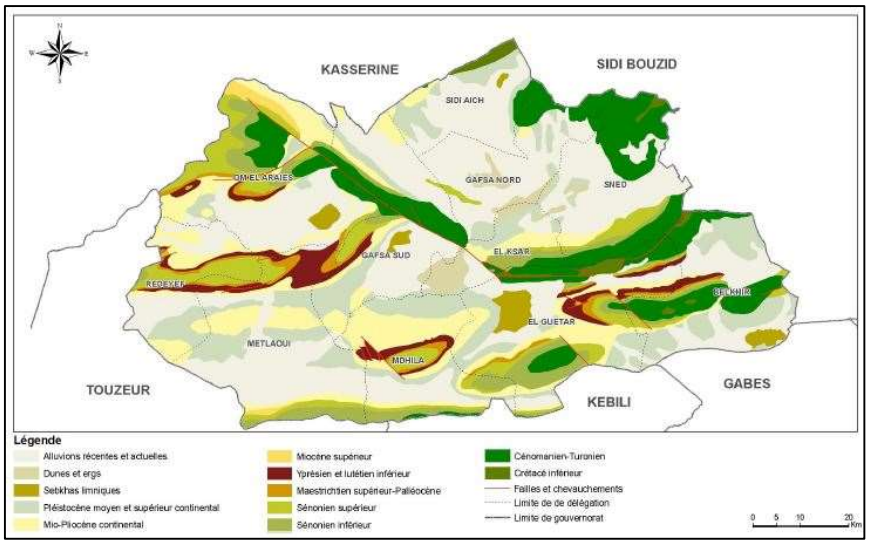

Fig 5 Geological map of the Gafsa Basin (ATLAS, 2014)

4.1.3. Reliefs

Figure 6 expresses a clear hypsometric contrast that varies between 1 and 1155m. This contrast presents two parts separated by main mountain ranges (Jalabia, Bou Ramli, Ben Younès and Orbata) crossing Gafsa Basin in the direction west-east. The first part is in the north. This part, which is characterised by altitudes exceeding 500m, is surrounded by the mountains of Jelabia, Bou Ramli, Ben Younes, Orbata, Goussa, Suinia and Sidi Aich. The second part is in the south. It can be identified by low altitudes of less than 250m and vast desert plains. This area is limited by the Jebels Morra and Bou Jerra in the south and by the Jebels Alim, Ben Younes and Orbata in the North.

The North Gafsa catchment area is divided into four regions according to hypsometric variation. The variation in altitude has a general tendency to increase from 260m to south-east towards 782m to the north-west. The first region extends over an area south-east of the watershed and is characterised by an altitude of less than 430m. The altitudes included between 430 and 490m characterize the second region. The third zone is identified by a very large surface area, to the north-west whose altitudes vary between 490 and 570m. As for the fourth, it extends over a limited area in the north-western part of the catchment, where elevations exceed 570m.

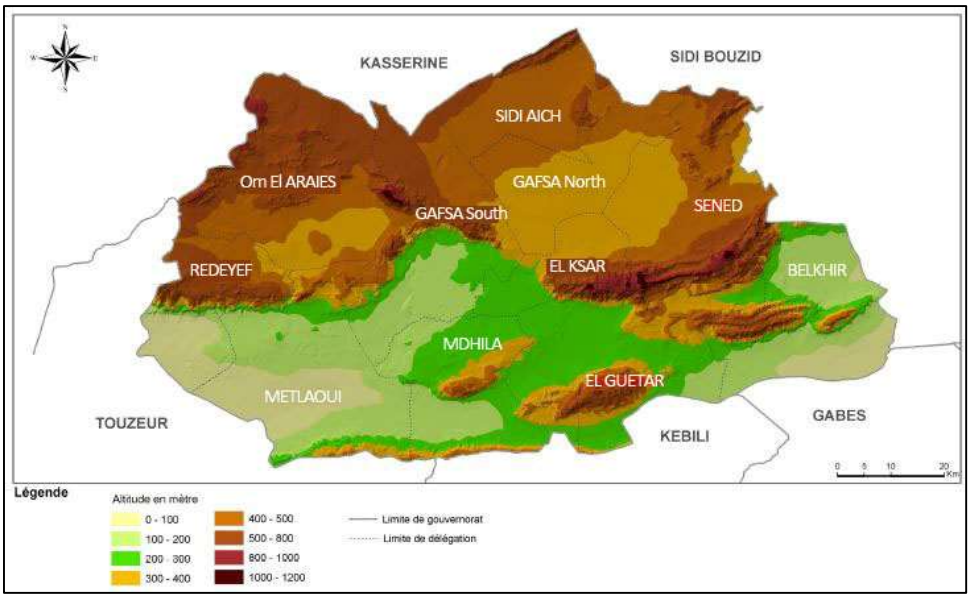

Fig 6 Geomorphology of GAFSA region (ATLAS, 2014)

4.1.4. Soils

The soils of Gafsa Watershed are mostly poorly developed and even limited to raw mineral soils, as is the case in the mountain ranges that cover a large part of the territory. The poorly evolved soils are found in limestone and gypsum formations and more particularly on the foothills of the mountains and isolated mountain in the lowlands and around wetlands (sebkhas and garaas), halomorphic soils are characterised by their high salt content (figure 7). Brown or reddish-brown isohumic soils are rare and extend to the north of the governorate (basin of Sidi Aïch) and in some intra-mountain depressions, north of Om El Araïes and around Redeyef. In the oasis of Gafsa, Lala and El Guetar, the soils are quite diversified and vary from poorly evolved coarse-textured soils to hydromorphic and halomorphic soils that pose drainage problems due to their saturation by irrigation water and insufficient drainage.

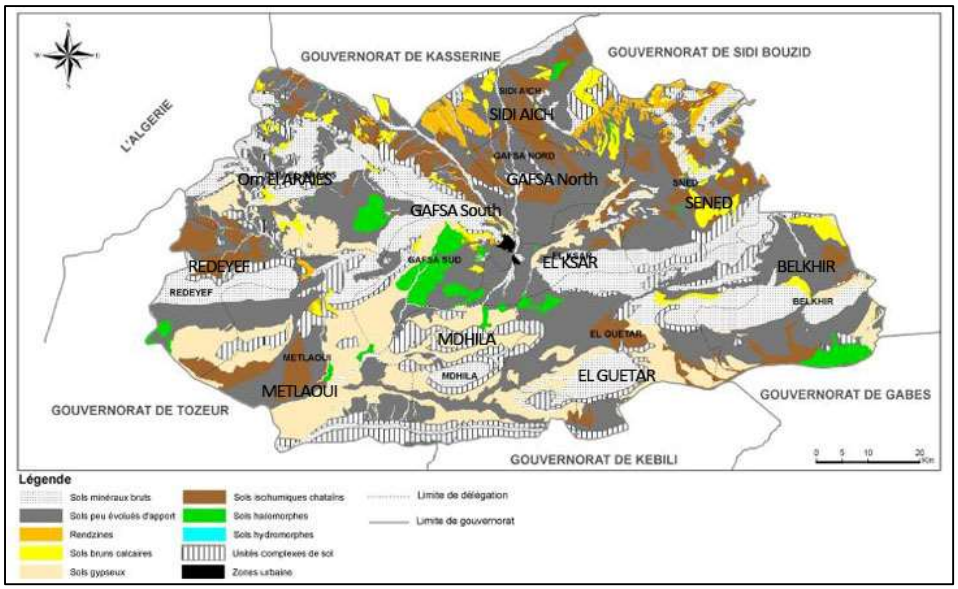

Fig 7 Soil map of GAFSA (ATLAS, 2014)

4.1.5. The plant cover

The vegetation map (figure 8), established in the National Atlas of Tunisia and shows a distribution of formations very marked by pedological and bioclimatic conditions. The typical formations of the Mediterranean-steppe domains and the pre-desertic steppe domains cover most of the territory. The Mediterranean-steppe domain is represented by the low matorral of rosemary and esparto grass which covers the jebel heights of the entire governorate. It is also represented by the sheet of esparto grass with white sagebrush which extends in a small zone in the south-west of the delegation of Sidi Aïch. The esparto sheet associated with the rural sagebrush is also found in the north of the governorate near Sidi Aïch and in Sidi Boubaker and Oum Lagsab (of the delegation of Om El Araïes).

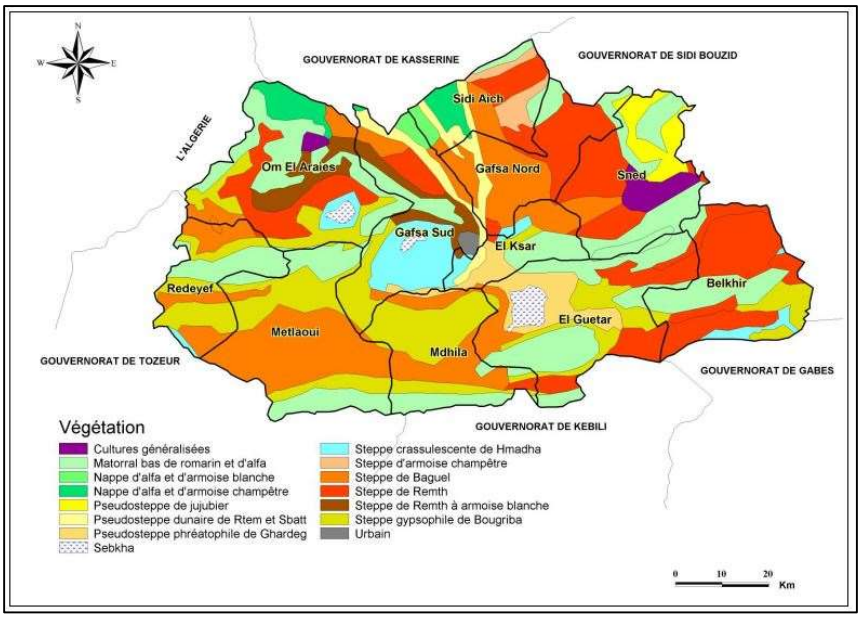

Fig 8 Land cover GAFSA region (ATLAS, 2014)

4.1.6. Hydrography

The hydrographic regime of Gafsa is endorheic, the wadis flow towards the sebkhas and chotts situated in the south of the mountainous chain of Gafsa (except for Garaat Sidi Aïch in the north) (figure 9). The most important sebkhas are from west to east: Garaat Douara in the centre of the mining basin, Chott El Guetar south of Jebel Orbata and Sebkhet Sid Mansour south of Jbel Belkhir.

Two large runoff areas can be distinguished:

1. The catchment areas of the large western wadis where the other ones flow from north to south: Oued Sidi Aïch, Oued el Kebir, Oued Bayache and Oued El Melah. To these main wadis which flow in the centre of the basin, are added, further west, the wadis of the mining basin, most of which flow into Garaat Douara. The others like Oued Thelja cross the jebels or go down their foothills towards the depressions and basins located in the south-west.

2. The watersheds of the small wadis to the east where the climatic and geomorphological conditions have not favoured the formation of major rivers. The most important wadis flow from the mountain ranges of Jbel Orbata, Jbel Chemsi towards the depressions near or far, such as Sebkhet Nouael where the waters of Oued Sarj and its tributaries flow or Sebkhet Sidi

Mansour for Oued Laoui-Oued Halfaya and its tributaries which flow down from the southern foothills of Jbel Berda.

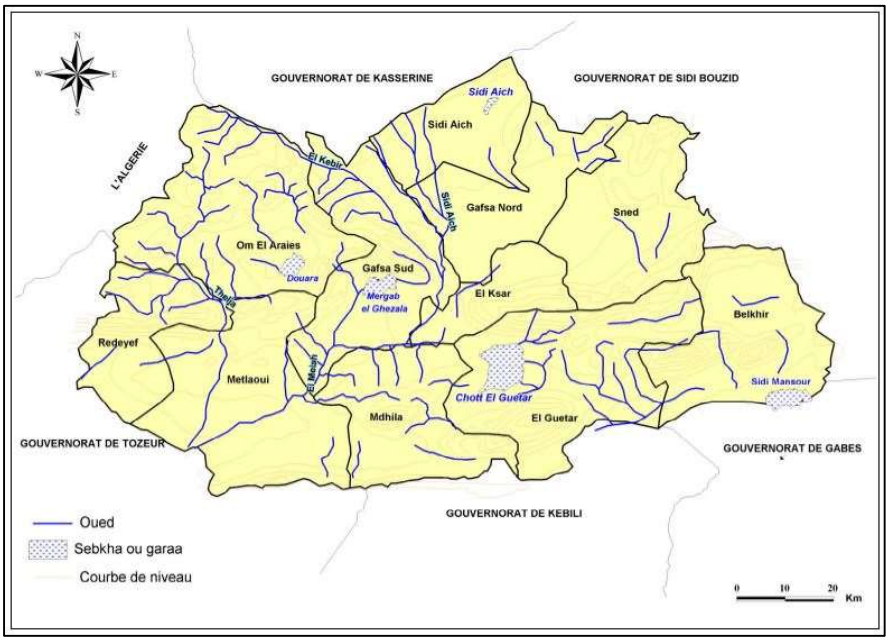

Fig 9 Hydrography of GAFSA Region (ATLAS, 2014)

4.2. DATA BANK

4.2.1. Source of data

The data were gathered from the publications of the General Directorate for Water Resources (DGRE) and the National Institute of Meteorology (INM), organisations responsible for the collection and publication of this information in Tunisia. Data are recorded at daily, monthly and yearly time intervals in 18 rainfall stations (Fig 10)

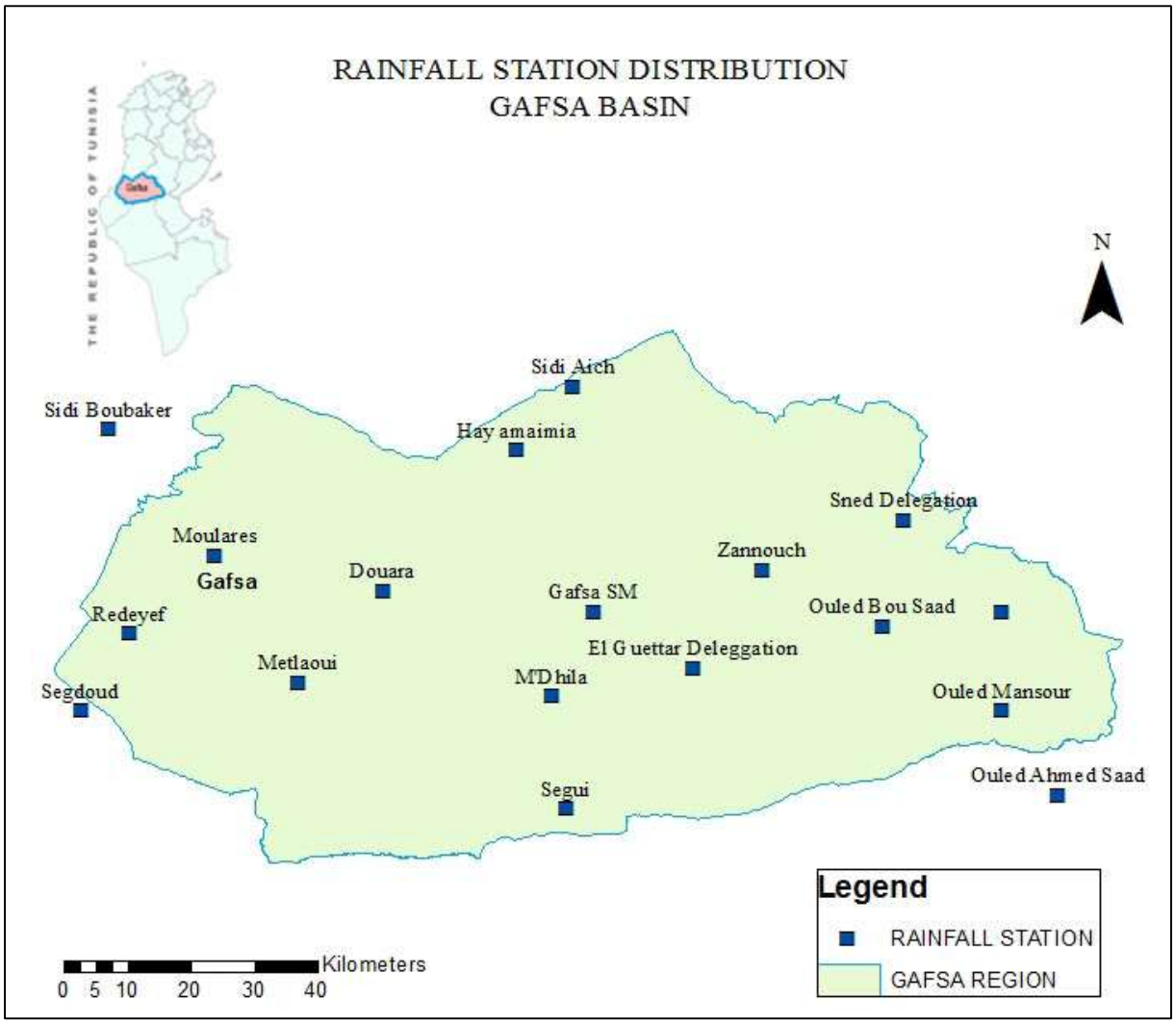

Fig 10 Rainfall stations distribution in Gafsa Basin

The choice of the stations used was not arbitrary but took into account the scale of the problem, the chronology of observations and the correct distribution over the entire catchment area in order to obtain a good presentation of climatic variations (Tab 3) presents the characteristics of the rainfall stations used and the corresponding time series.

TAB 1 Characteristics of rainfall stations and series (CRDA-Gafsa, 2015)

Nbr	Name of station	Latitude (Dec)	Longitude (Dec)	Altitude (Dec)	Average Precipitation (mm)	Recording period	Record length
1	Gafsa SM	34.41	8.81	300	167.4	1960-2015	56
2	Redeyef	34.38	8.15	568	153.9	1960-2015	56
3	Moulares	34.49	8.27	480	135.1	1960-2015	56
4	Metlaoui	34.31	8.39	202	110.8	1960-2015	56
5	Sidi Aich	34.73	8.78	550	211.9	1960-2015	53
6	Sned Delegation	34.54	9.25	429	199.0	1960-2015	56
7	M'Dhila	34.29	8.75	270	111.9	1960-2015	56
8	El Guettar Deleggation	34.33	8.95	228	135.6	1960-2015	56
9	Sidi Boubaker	34.67	8.12	500	176.1	1963-2015	53
10	Ouled Mansour	34.27	9.39	100	125.8	1963-2015	53
11	Haouel El Oued	34.41	9.39	150	128.1	1979-2015	37
12	Ouled Bou Saad	34.39	9.22	770	149.4	1979-2015	37
13	Zannouch	34.47	9.05	374	160.7	1976-2015	34
14	Ouled Ahmed Saad	34.15	9.47	392	159.5	1997-2015	19
15	Hay amaimia	34.64	8.70	469	149.9	1997-2015	19
16	Douara	34.44	8.51	388	109.4	1997-2015	19
17	Segdoud	34.27	8.08	38	93.9	1997-2015	19
18	Segui	34.13	8.77	38	117.3	1982-2015	34

4.2.2. CLIMATIC CONTEXT OF THE STUDY AREA

4.2.2.1. Monthly temperature

The region of Gafsa is characterised by an arid climate with high temperatures. Based on the thermal data recorded at the Gafsa weather station during the period 1960-2014, the average monthly temperature is 19.2°C. The lowest temperature is detected in December 1980 (6.8°C) while July 2003 is the hottest month (32.7°C) (figure 11).

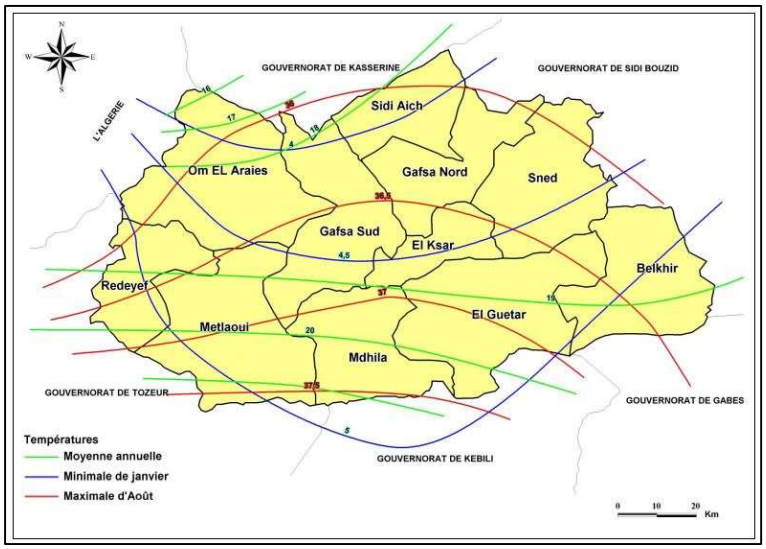

Fig 11 Temperatures variation in GAFSA (ATLAS, 2014)

4.2.2.2. Evapotranspiration and humidity

Average annual evapotranspiration. estimated at the weather station of Gafsa. is of the order of 2488mm. This value is distributed in 299; 438; 767 and 984 mm in the winter. spring. summer and fall seasons respectively. With regard to humidity. the region is characterised by relative humidities in the order of 55%; 46%; 36% and 44% in winter. spring. summer and autumn successively (SMG, 2014).

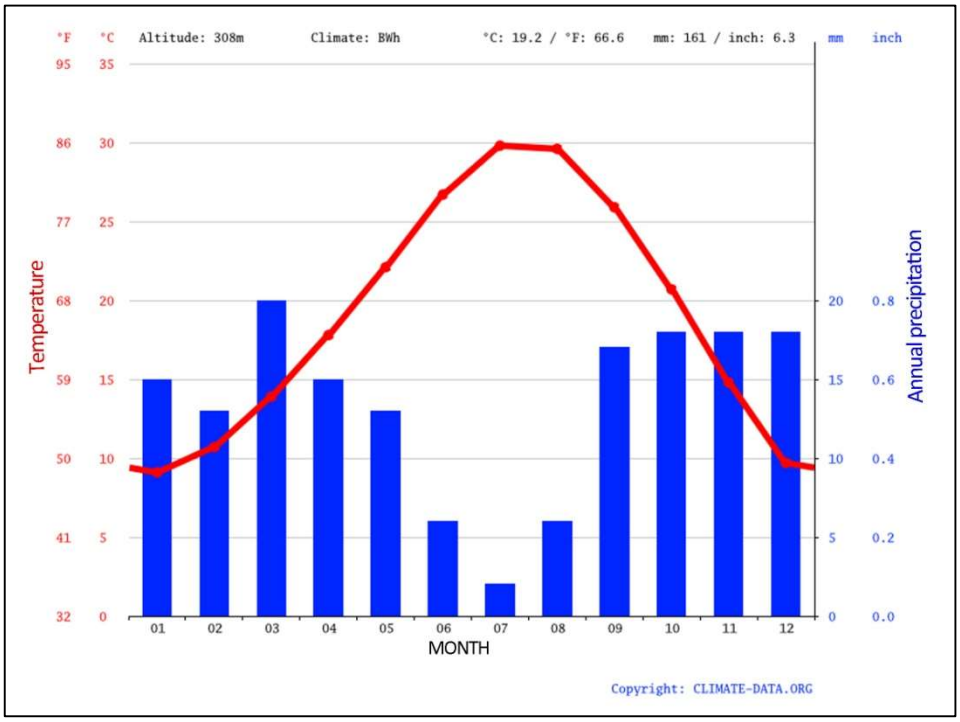

Fig 12 Monthly rainfall distribution (ATLAS, 2014)

CHAPTER FIVE

SPATIAL AND TEMPORAL STUDY OF RAINFALL VARIABILITY

Introduction

It is necessary to check the data for continuity and consistency before using the rainfall data in any hydrologic analysis. This is due to the fact that the recorded data might be erroneous due to wind effects, changes in station environment, errors while observing the data and many more. Furthermore, data are usually checked in order to test the validity of the rainfall data it self. There are various analyses that can be conducted to analyse the rainfall data. namely the independence test, stationary test and homogeneity test (Rao and Kao, 2006).

5.1. Preliminary tests:

5.1.1. Independence test

This is a test to verify that the probability of occurrence of an observation in a sample is not affected by any other observations in the same sample. A data series is temporally independent if no observation in the series has an influence on the observation that follows it. Data dependency varies according to the interval between successive items in a series. Indeed, independence can be measured by the significance of correlation between N-1(N sample size) pairs of the i^{th} and $(i+1)^{th}$ observation. The obtained correlation coefficient tends towards zero, implying **independent** data series.

5.1.2. Stationarity test

This test is applicable in order to verify that the characteristics of the data set are invariant over time. The test is also called a trend test. The correlation coefficient of the Spearman test is used to check the trend of the series.

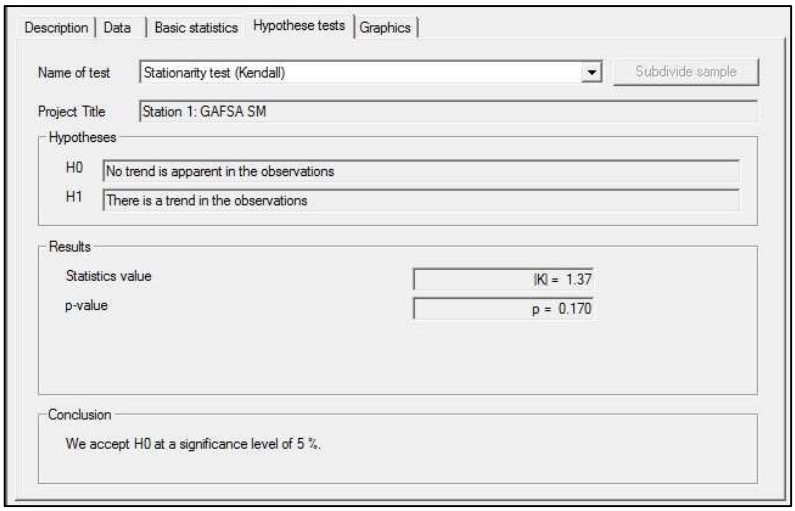

Fig 13 Stationarity test

➔The correlation coefficient tends towards zero, the data are: homogeneous, random and without bias for a level of significance of 5%

5.1.3. homogeneity test

A sample is said to be homogeneous when all its observations come from the same statistical population. The homogeneity test is carried out using the Mann-Whitney test. The latter depends on the size of the samples and their corresponding ranks.

➔The correlation coefficient tends towards zero, sample is said to be homogeneous

A preliminary statistical study of the rainfall data was first established. Indeed, the series of observations must be independent, random, homogeneous, and without tendency. These hypotheses were verified using the HYFRAN Software. The considered tests were accepted at a significance level of 5%.

5.2. Data fitting:

5.2.1. Introduction

Probability distribution analysis is applied to analyse the rainfall data for the computation of expected rainfall of a given frequency (Dawood, 2009). It is defined as the statistical analysis of a random variable. The most frequently used Probability Distribution Functions include normal, log-normal, and Pearson Type 3 distributions. Fitting of these frequency distributions will be carried out using the method of maximum likelihood to identify the probability of event occurrence. The three PDF used in the study namely; Normal distributions, Log Pearson Type 3 and Generalized Extreme Value (GEV) distribution and the selection of the PDF from recommended by the previous studies for annual maximum rainfall estimates.

5.2.2. Normal distribution

The normal distribution or also known as Gaussian distribution is applied to symmetrically distributed data. Besides, it is also referred as the bell curve due to the bell shape of distribution (Kwaku and Duke, 2007). The normal distribution can be specified by two parameters, namely mean (μ) and standard deviation (σ). The data will fall between two real numbers with non-zero over the entire line. (j.Eng.Applied sci, 2016)

5.2.3. Log-Pearson Type 3 distribution

The log-Pearson type 3 is extensively used for hydrological project in USA (Ewemoji and Ewemooji, 2011). The concept of this distribution is to transform the variation into logarithmic form and then the transformed data are further analysed.

5.2.4. GEV Distribution

The theory of extreme value was first developed in 1927 for independent and identically distributed random variables (Shukla et al., 2012). The simplest three forms of the extreme value distribution are given by the Gumbel, Frechet and Weibull families or also known as type 1-3 respectively. However, due to the problem of determining which of the distributions should be used to analyse a data set, the GEV was developed. There are three parameters of GEV namely scale, location and shape.

5.2.5. Goodness-of-fit test

In order to evaluate the quality of the fitted distributions, the goodness-of-fit test was conducted. It represents the statistical hypothesis used to evaluate if the input data is an independent sample from a particular distribution. The goodness-of-fit test can be measured using Chi-square test which is one of the tests to compare the input data histogram with the fitted distribution. Data were first divided into K-class intervals whereby in the study K≈$\sqrt{n}$ where n is the number of total recorded years.The average of values in any group should be >5. The goodness-of-fit tests were conducted at 5% level of significance.

From the Chi-square test (x^2), it can be conducted that if the observed frequencies are close to the corresponding expected frequencies, it representing a good fit or otherwise, it is a poor fit. The hypothesis made is that a good fit leads to acceptance of H0 whereas the data is said not to follow the specified distribution for a poor fit that leads to a rejection. The samples of the graphic output for each PDF fitting is shown in fig 14, 15 and 16 respectively. The graphs show the best-fitted PDF to describe the rainfall was indicated by the annual maximum rainfall data that lay within the lower and upper limit of control bands of 95% confidence intervals. Figs 13 and 14 show that some of the annual maximum rainfall data were not laid within the lower and upper limit of control bands set up which is 95%. Thus, the 95% confidence level was not achieved.

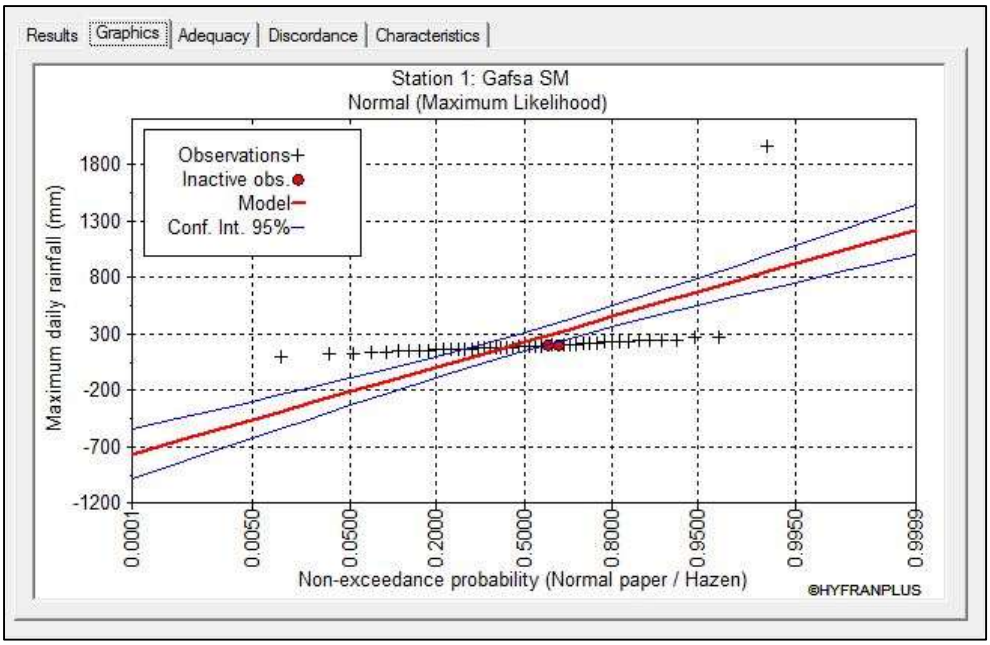

Fig 14 Normal distribution

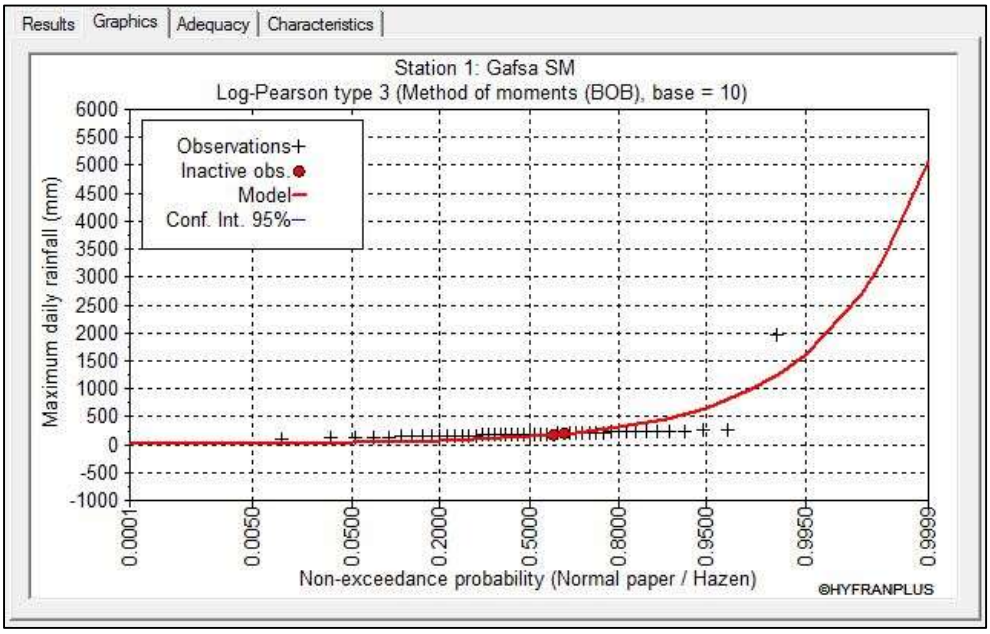

Fig 15 Log-Pearson Type 3 distribution

However, as shown in Fig 16, it is clearly seen that all the annual maximum rainfall data lie within the lower and upper limit of control bands. This clearly shows that GEV represents the best-fit distribution for GAFSA SM rainfall station at a 95% confidence level.

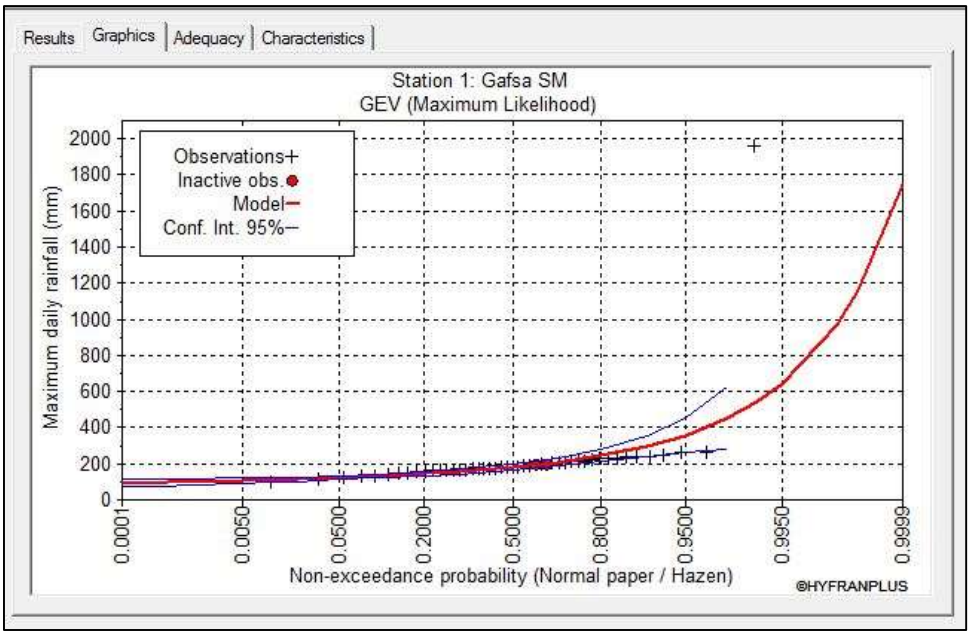

Fig 16 GEV distribution

A summary of Chi-square test for each of the PDF is shown in Table 4. The p-value for REDEYEF STATION is 0.0003 for the normal distribution and 0.0031 for Log-Pearson Type 3, which are both less than 0.05. Therefore, the null hypothesis (H_0) can be rejected at a significant level of 5%, and also indicates that the underlying distribution of this sample is neither Normal nor Log-Pearson Type 3.

TAB 2 the Chi-squared Test

Probability distribution function fitting

Station name	Normal		Log-Pearson Type3		**GEV**	
	x^2	p-value	x^2	p-value	x^2	p-value
GAFSA SM	1.73	0.7847	5	0.1718	1.73	0.6295
REDEYEF	21.33	**0.0003**	13.87	**0.0031**	7.33	**0.062**
ZANNOUCH	1.27	0.867	1.73	0.6295	1.73	0.6295
SIDI AICH	4.07	0.3971	3.6	0.308	3.6	0.308
Average	7.1	---	6.05	---	**3.5975**	---

The p-value is 0.0620 for GEV pdf that is >0.05. Thus, the null hypothesis was accepted at a significant level of 5% and also indicates that the underlying distribution of this sample is GEV. The same analysis was performed on the other three stations by using the same methods to identify the best-fit distribution. The smallest average value of Chi-square test for the GAFSA

BASIN is 3.5975 for GEV distribution which indicates that GEV is the best-fit PDF to describe rainfall pattern in the basin.

5.2.6. Conclusion

In conclusion, the rainfall data analysis in the GAFSA BASIN using HYFRAN-PLUS yielded acceptable results. All the rainfall data are independent, stationary and homogenous. Three probability distribution functions were considered for possible fit to rainfall data. The best fitted distribution, which yielded the smallest Chi-square value x^2 (3.6), was shown to be GEV. This latter represents the best PDF for the annual maximum data taken from the four stations in the upper part of the GAFSA BASIN.

5.3. Descriptive analysis

5.3.1. Descriptive statistical analysis of the rainfall data sets

A descriptive statistical study of the annual rainfall series is established for the GAFSA basin. The average, minimum and maximum rainfall, as well as the statistical characteristics (median, standard deviation, coefficients of variation, skewness and kurtosis) are presented in the (table 5).

TAB 5.1 Statistical characteristics of rainfall in the study area

Station Number	Altitude(m)	Longitude	Latitude	Standard Deviation (mm)	Median (mm)	CV %	Skewness	Kurtosis
1	300.00	8.81	34.41	227.33	169.75	0.34	0.04	0.06
2	568.00	8.15	34.38	306.88	217.00	0.41	0.06	0.06
3	480.00	8.27	34.49	231.58	195.05	0.19	0.05	0.06
4	202.00	8.39	34.31	182.43	133.00	0.37	-0.01	0.08
5	550.00	8.78	34.73	656.05	503.60	0.30	2.01	2.50
6	429.00	9.25	34.54	375.54	305.95	0.23	0.11	0.07
7	270.00	8.75	34.29	310.42	219.50	0.41	0.06	0.06
8	228.00	8.95	34.33	203.93	165.20	0.23	0.04	0.06
9	500.00	8.12	34.67	248.76	225.90	0.10	0.06	0.06
10	100.00	9.39	34.27	143.58	223.98	0.64	0.06	0.06
11	150.00	9.39	34.41	196.86	225.70	0.87	0.06	0.06
12	770.00	9.22	34.39	345.67	394.18	0.88	0.50	0.40
13	374.00	9.05	34.47	368.33	282.95	0.30	0.08	0.06
14	392.00	9.47	34.15	167.58	178.50	0.94	0.05	0.06
15	469.00	8.70	34.64	116.07	177.43	0.65	0.05	0.06
16	388.00	8.51	34.44	140.71	120.50	0.17	-0.04	0.10
17	38.00	8.08	34.27	125.87	107.00	0.18	-0.08	0.12
18	38.00	8.77	34.13	207.89	158.00	0.32	0.03	0.06

The positional parameters such as the arithmetic mean and the median are intended, in the case of a quantitative characteristic, to characterise the order of magnitude of the observations and the central tendency. Whereas the dispersion parameters concern the standard deviation, the coefficient of variation, the coefficient of asymmetry (skewness), and the kurtosis coefficients whose objective is to characterise the variability of the data in the sample. The standard deviation (σ) measures the dispersion of a series of values around their mean and

the coefficient of variation (CV) measures the degree of variability of the variable studied in a series and the dispersion of values in relation to the mean.

The coefficient of variation (CV) is a statistical measure of the dispersion of data points in a data series around the mean. The coefficient of variation is the ratio of the standard deviation to the mean. It is a useful statistic for comparing the degree of variation from one data series to another, even if the means are totally different from each other.

Skewness refers to a distortion or asymmetry that deviates from the symmetrical bell curve, or normal distribution, in a set of data. If the curve is shifted to the left or to the right, it is said to be skewed. Skewness can be quantified as a representation of the extent to which a given distribution varies from a normal distribution.

Kurtosis is a statistical measure that is used to describe distribution. Whereas skewness differentiates extreme values in one versus the other tail, kurtosis measures extreme values in either tail. Distributions with large kurtosis exhibit tail data exceeding the tails of the normal distribution (e.g., five or more standard deviations from the mean). Distributions with low kurtosis exhibit tail data that are generally less extreme than the tails of the normal distribution.

The standard deviations of annual rainfall indicate high inter-annual variability in the GAFSA catchment. The standard deviations are higher than 116 mm per year and sometimes reach more than 656 mm per year (Table 5).

According to Figure 17, there is an alternating increase and decrease in the rainfall trend across the study area. A maximum of 967 mm at station No. 5 in the extreme north-east and a minimum of 0 mm in stations No. 7 and 2 in the south and south-west respectively.

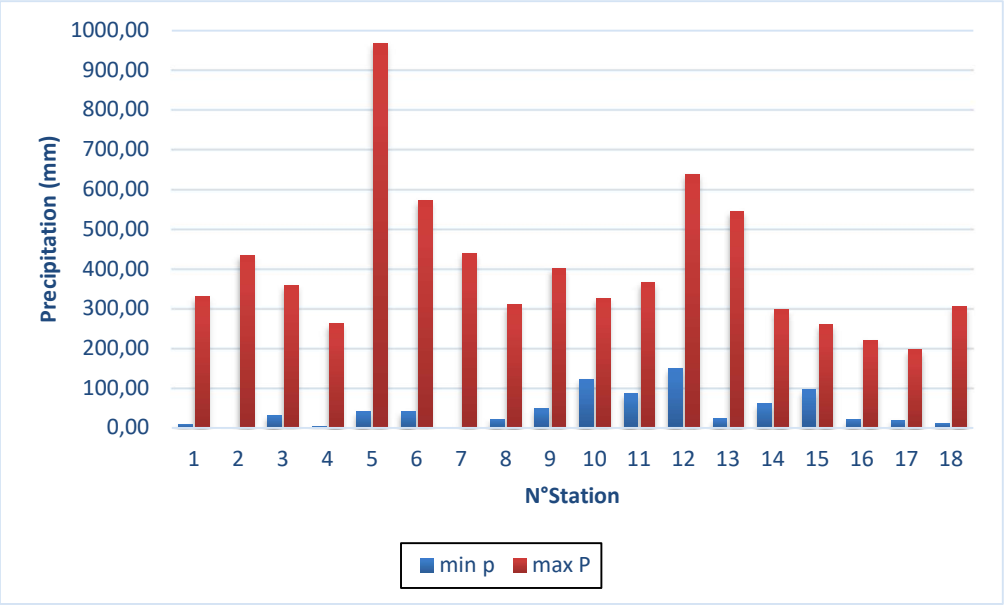

Fig 17 Variability of minimum and maximum rainfall

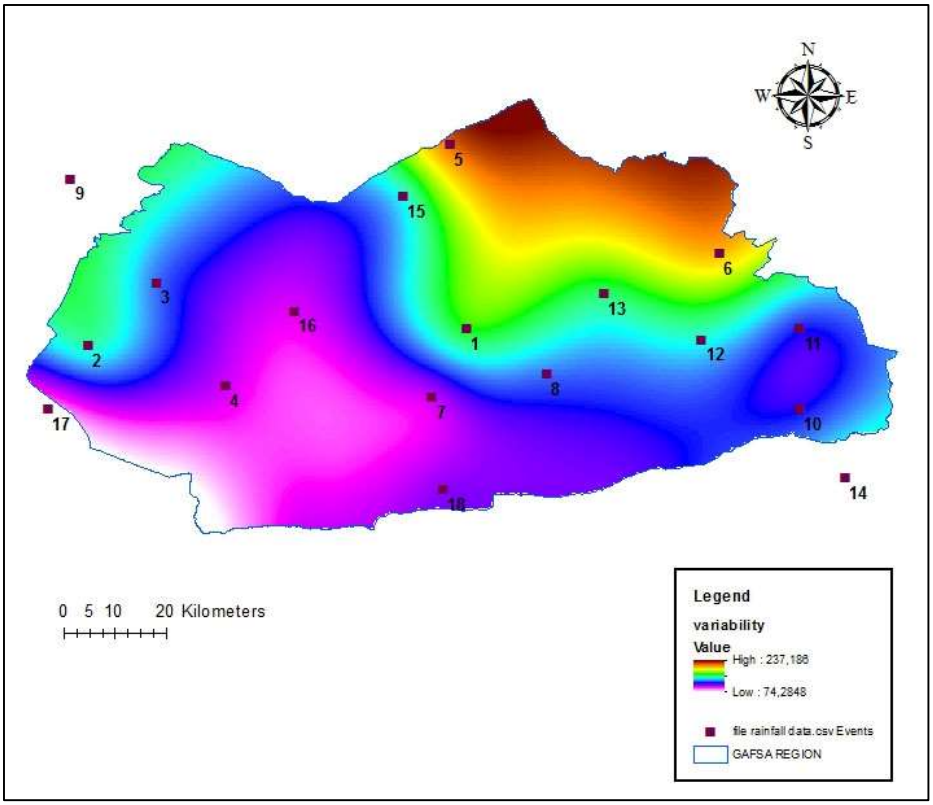

Fig 18 Distribution of the average annual rainfall in the GAFSA catchment area

Figure 18 shows that the distribution of average annual rainfall across the study basin is not uniform. Significant variability in the north and north-west compared to the south in both directions east and west where the rainfall amounts gradually decrease towards the south.

Average rainfall in the study basin varies between 237 mm (550 m Altitude) in station 5, located in the north eastern, to less than 74 mm (38 m Altitude) in station 17, situated in the extreme west (Fig 18). The important values of average annual rainfall are recorded at stations (1, 5, 6, 12, 13 and 15), characterized by high latitudes. Rainfall increases from south to north and west to east, characterized by a mountainous relief.

These results show that rainfall variability in the GAFSA basin is influenced by the effect of the topography in the eastern and north eastern regions. Indeed, these mountains placed along the North play the role of a climatological barrier which favours more precipitations when moving away from the west side. Thus, it can be concluded that for high rainfall, the variability is important but remains local, this result suggests that rainfall trends can be attributed to local changes. Rainfall variability in the GAFSA basin is influenced by the effect of topography in the north-eastern regions, while in the south-western regions other factors such as latitude, longitude, proximity to mountains and wind speed direction affect the characteristic precipitation and are the main sources of variation.

- **Dispersion**

The statistical characteristics of rainfall during the period 1961-2014 such as coefficient of variation (CV), coefficient of skewness (CS) and coefficient of kurtosis (Ck) are presented in (table 5). The mean values of CV, CS and Ck for the study area are 0.42, 0.18 and 2.34, respectively. The CV values are generally higher than 25%, except for stations 4, 10, 17 and 18, which are located in the south-eastern and south-western regions (low altitudes).The CV values obtained show a large variation. They vary from 10% (station 10) to 94% (station 15), which means a significant increase from South to North and from the West to East directions.

The values of (CS) for all-time series are generally positive. They are close to zero for most stations. The maximum Skewness value 2.01 recorded in (station 5) which is again located in the north-eastern part of the region (table 5).

The maximum value for the different statistical parameters CS, and Ck was obtained for station No. 5 (mountainous region). The values of (Ck) for most stations vary between 0.06 and 0.12 (table 5). The exception is station No. 5 with a (Ck) value close to 3, indicating that low rainfall is more frequent than high rainfall (Amrutha and Shreedhar, 2014).

Skewness coefficients for most of the stations are positive, indicating that low rainfall happens frequently while high rainfall amounts occur rarely. For some of the stations, skewness coefficient values are equal to or nearly equal to zero, indicating that data follow a normal distribution.

In general, the coefficient of variation CV decreases slightly, the coefficient of skewness CS remains constant and the coefficient of kurtosis Ck increases slightly with increasing annual rainfall. These results are in agreement with those found in the work of (Modarres and Rodrigues da Silva, 2007 and Ellouze, 2010).

- **Regression**

The study of the regression of precipitation with latitude, altitude and longitude (Figures 19, 20 and 21) shows that there is a correlation with latitude and longitude. A significant correlation between altitude and average precipitation is obtained.

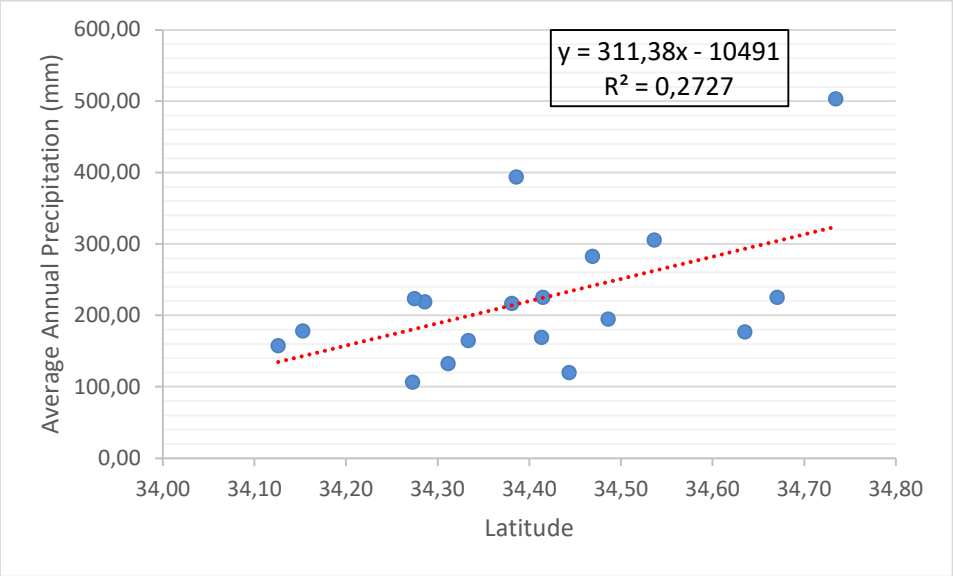

Fig 19 Variation of average rainfall with latitude

Average annual rainfall increases from north (Altitude is high) to south (Altitude is low). However, there are stations with fairly high altitudes and high rainfall (Table 5 and Fig 17). These are located between the mountains along the north and north east. Mountains play again a

role of a climatological barrier, which favours more rainfall. Similar to longitude, values of correlation coefficients between rainfall and altitude are low, except for the eastern zone, characterized by relatively higher values (Figure 32).

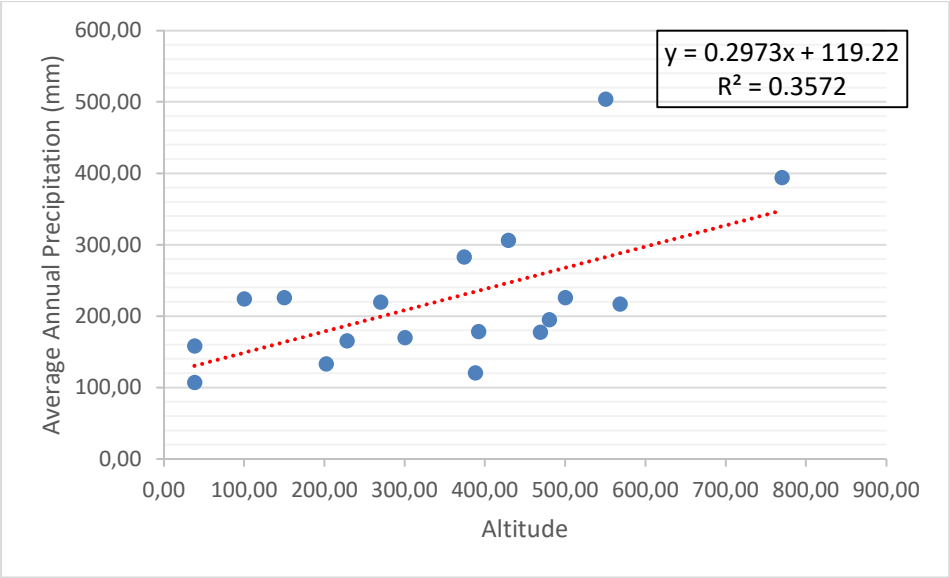

Fig 20 Variation of average rainfall with altitude

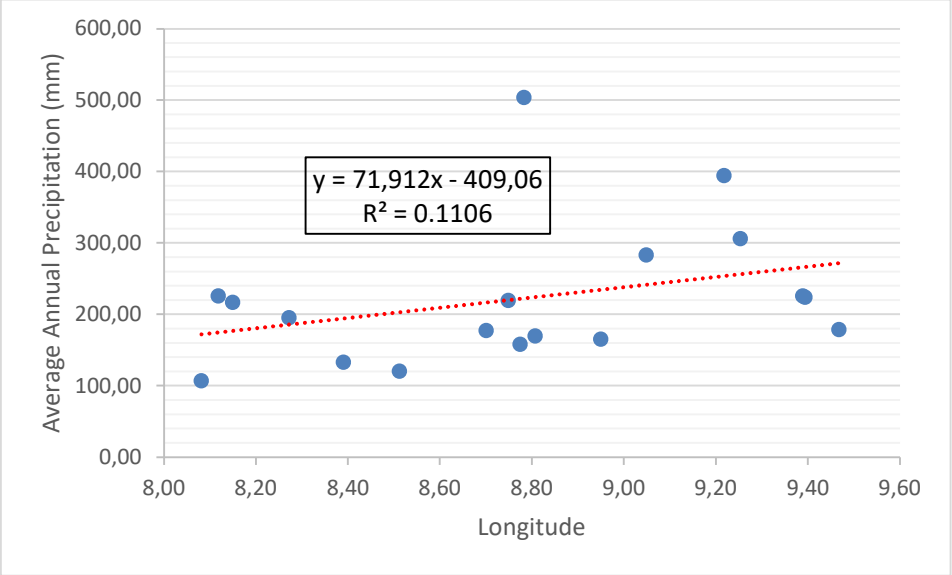

Fig 21 Variation of average rainfall with longitude

5.4. Subdivision of the Gafsa watershed:

5.4.1. Subdivision based on PCA

The principal component analysis applied to annual series of rainfall recorded during 55 years (1960-2015) for the 18 rainfall stations distributed in the basin. The considered variables for PCA study are the average annual rainfall, altitude, longitude, latitude and the average monthly precipitation. The projection on the factorial plan (1x2), which explains 77% (Table 6) of the inertia of all variables and selected individuals, brings out 4 zones reflecting different climatic and physiographic characteristics (figure 22) .

TAB 5.2 Total explained variance

Component	Initial Eigen values		
	Total	% variance	%Cumulative
1	2.738	54.768	54.768
2	1.136	22.729	77.497
3	0.665	13.297	90.794
4	0.335	6.709	97.503
5	0.125	2.497	100.000

The first group G1 (Fig 22) stations (6, 12 and 13) are all situated at the northern part of the basin and characterized by high altitudes varying between 374 and 770 meters above the sea level. It is a mountain range, characterized by high altitudes, which act as a topographical barrier, contributing to orographic precipitation; forcing moist air to rise which depends on altitude, slope and its orientation.

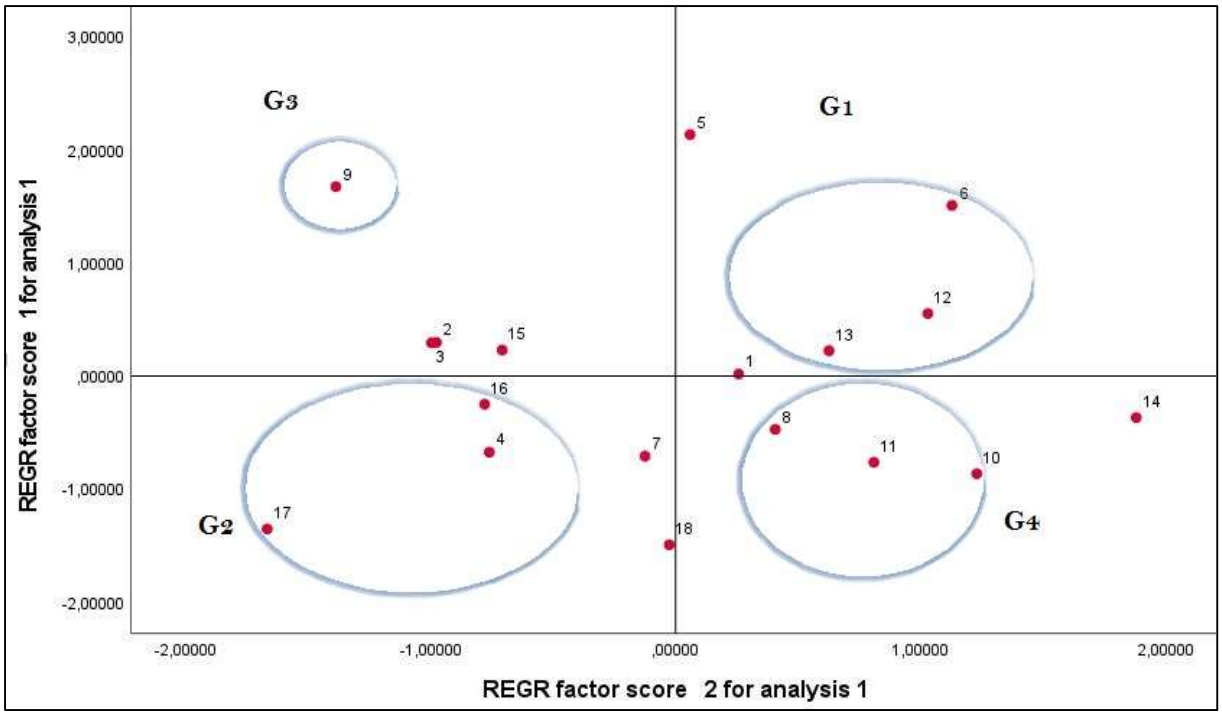

Fig 22 Scatter plot of rainfall stations by PCA

The second group G2 stations (4, 16 and 17) are located in the southern part of the basin and characterized by low altitudes varying from 38 to 388 meter above the sea level. The position of this zone is specified by the domination of lowest altitudes therefore flat area which famous the variability and the importance of precipitation. One single station (the 9th form the third group G3) is located in the extreme North West with an altitude of 500 meter above the sea level. This group may ensure the transition between highest and lowest variability in the basin

The forth group G4 contains 3 stations (8, 10 and 11) and their altitudes are respectively 228, 100 and 150 meters above sea level. A flat area, situated in the eastern part of the study area, is also distinguished. These four groups show the influence of relief through the presence of mountain ranges, the effect of proximity to the sea, and the impacts of rainfall seasonality. However, the distribution of rainfall is closely related to altitude, distance from the sea to the rain gauge stations and seasonality compared to latitude. This relationship is due to the irregularity of rainfall and seasonal changes.

The average altitude is 347 m, varying from a minimum of 38 m to 770 m. The existence of stations characterised by high altitudes and low average rainfall indicates that there are other factors that influence rainfall variability (Fig 23).

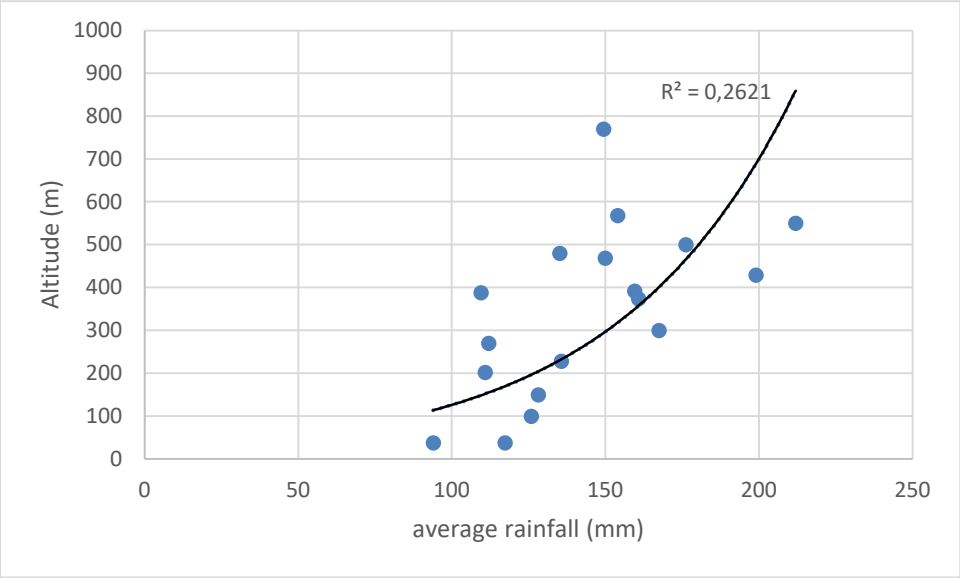

Fig 23 Variation of average rainfall with altitude

Therefore, altitude is not the only factor that characterises annual rainfall, which increases from south-west to north-east, involving an important effect of longitude (rainfall increases from the top where longitude is high to the mainland where longitude is low). However, there are stations with fairly high longitudes and high rainfall. These are located close to the top of the mountain (stations: Sidi Aich (st 5) (long 8.78 m, alt 550 m and average rainfall 967 mm), Ouled Bou Saad (st 12) (long 9.22 m, alt 770 m and average rainfall 638 mm)).

The trend line of the average rainfall versus altitude gives a coefficient of determination R^2 equal to 0.39 (Fig 23). This coefficient is very low showing that the relationship between these two parameters is impulsive. Similarly, the study of the spatial distribution of precipitation, based on the quality of representation (Tab 7), shows that the best quality coincides with latitude (0.42) and average rainfall (0.99) while the contribution of altitude is (0.39). It can therefore be concluded that altitude is not the main factor in the spatial variability of precipitation and its contribution remains small and limited, whereas longitude and latitude have a significant effect on precipitation.

TAB 5.3 Quality of representation

	Quality of Representation
Altitude	0.39
Longitude	0.05
Latitude	0.42
Average Rainfall	0.99

5.4.2. Subdivision based on the cumulative rainfall index

The shape of the cumulative rainfall index (CRI) variation curve was examined for each station belonging to the study catchment. The general trend of these curves is used to divide the study area into regions with the same characteristics of temporal variations of precipitation. Six classes/groups are defined according to the shape of the variation curves of the cumulative rainfall index (Figs 24 to 29).

The first group, with 6 stations (Sidi Aich, Sned, Sidi Boubaker, Zannouch, Hay Amaimia and Ouled Ahmed Ben Saad), is characterised by an almost linear trend during the period (1960-1989) separated by two increasing trends during the periods (1969-1971 and 1989-1992) and the variation start to alternate positively and negatively from 1997 to 2014.

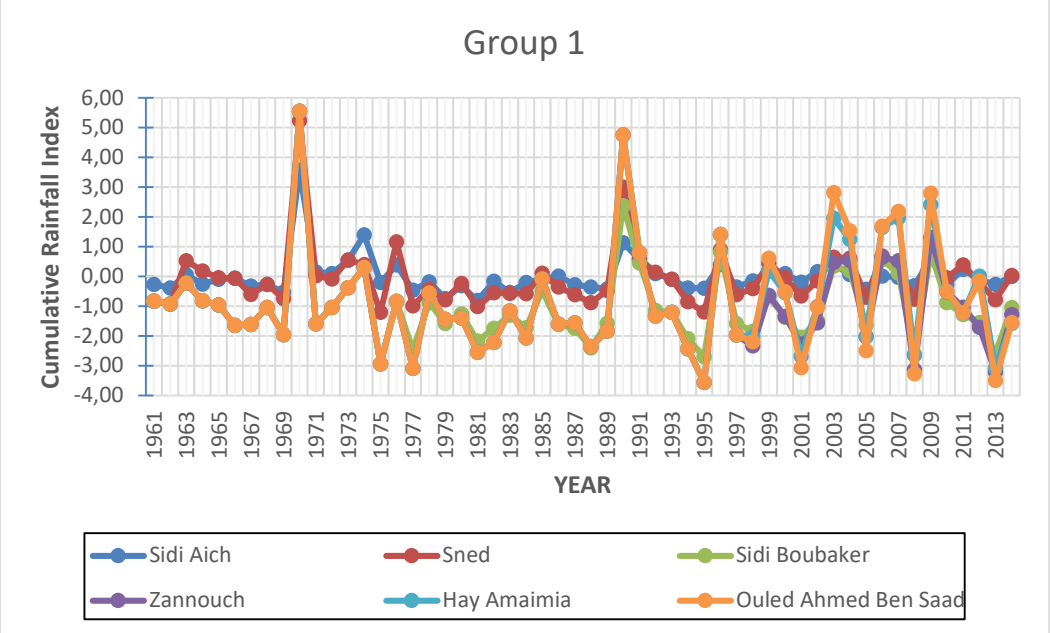

Fig 24 Annual variation of the cumulative rainfall index in group 1

Second group, only one single station which is characterised by an alternation of increasing and decreasing trend during all the recorded period from 1961 to 2014 with a minimum cumulative rainfall index observed in 2008 and a maximum in 1997.

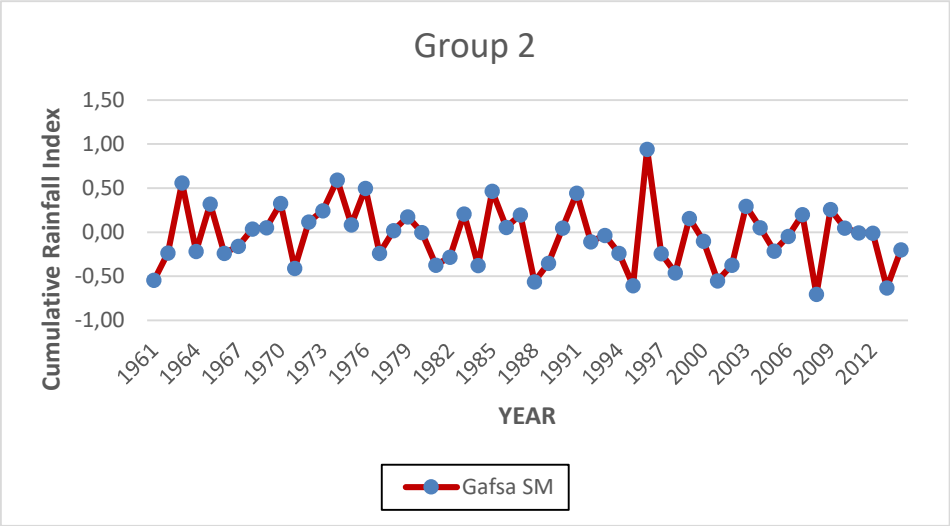

Fig 25 Annual variation of the cumulative rainfall index in group 2

Three stations (Segdoud, Metlaoui and El Guettar) form the third group, characterized by two parts of variability. First, from (1961 to 1991) an almost linear trend including two peaks in 1970 and 1990 respectively. The second part, from (1991 to 2011) an increasing alternating trend, with a maximum observed in 2010.

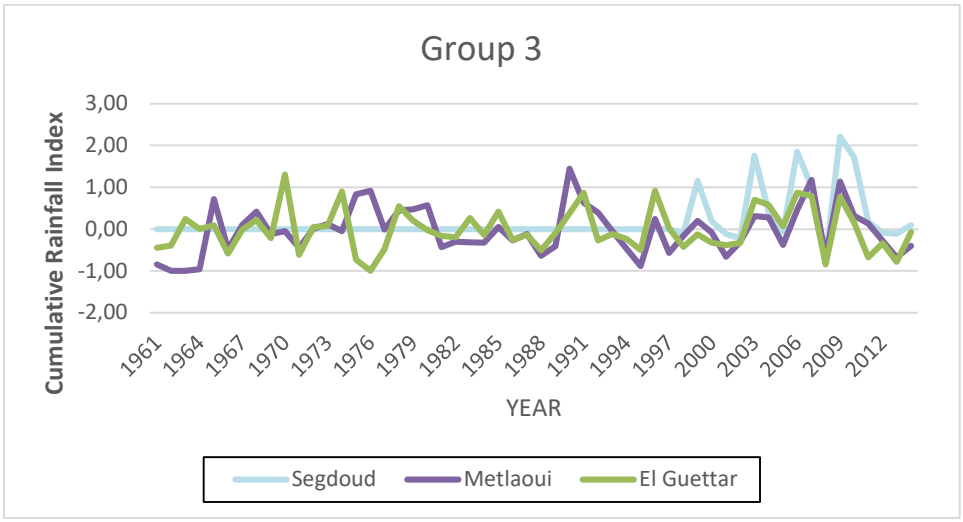

Fig 26 Annual variation of the cumulative rainfall index in group 3

The forth group includes 3 stations (Ouled Mansour, Haouel el Oued and Ouled Bou Saad). From (1961 to 1979) a linear negative trend in variation then start to increasing gradually from 1980 to 1991 to reach a peak in 1991, then decreasing but it keep alternating from 1991 to 2014 with a maximum cumulative index observed in 2007 and a minimum index in 1995.

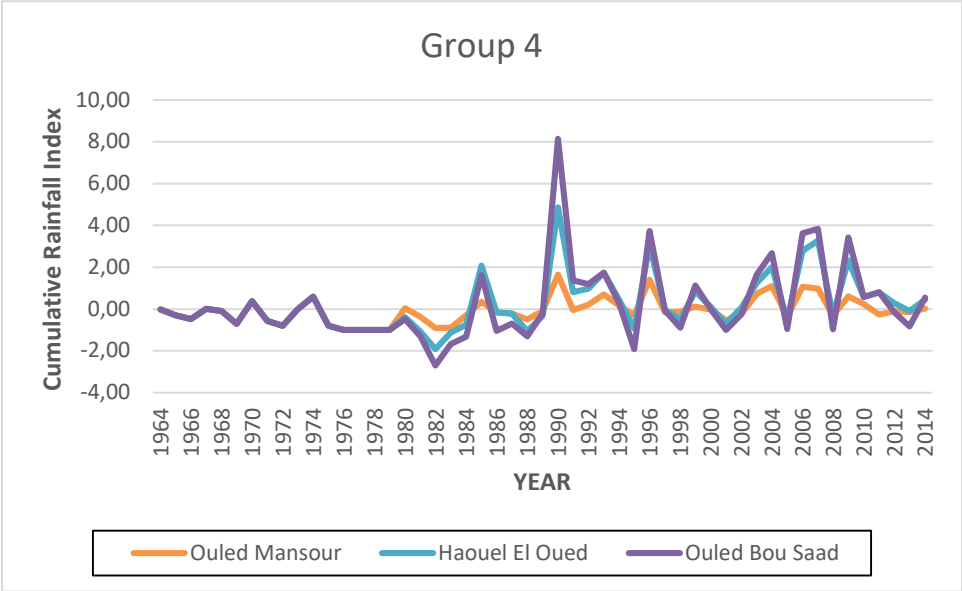

Fig 27 Annual variation of the cumulative rainfall index in group 4

Group 5 includes stations (Douara, Redeyef and Moulares). From (1961 to 1990) the trend is alternating symmetrically with a maximum in 1970 and a minimum reached during the period 1978 to 1981. The second trend characterized by an increasing trend of variation including two peak reached respectively in 1990 and 1997.

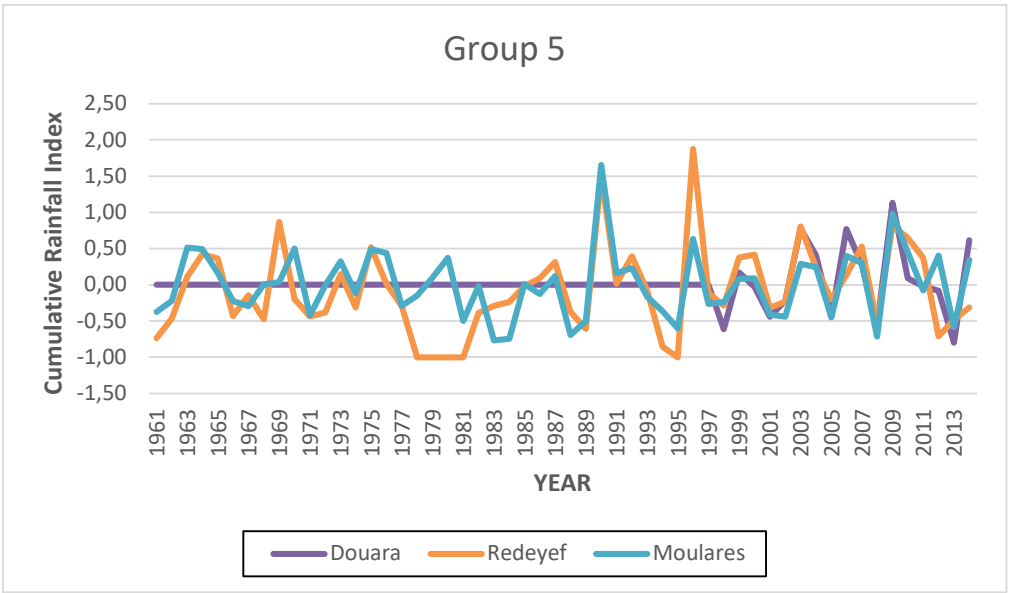

Fig 28 Annual variation of the cumulative rainfall index in group 5

The sixth group is represented by only two stations. Two parts characterise the trend. From 1961 to 1982, the trend is negative with a minimum reached in 1974. The second trend, which is positive starts to increase gradually from 1988 and continues alternating positively to reach a maximum in 1991.

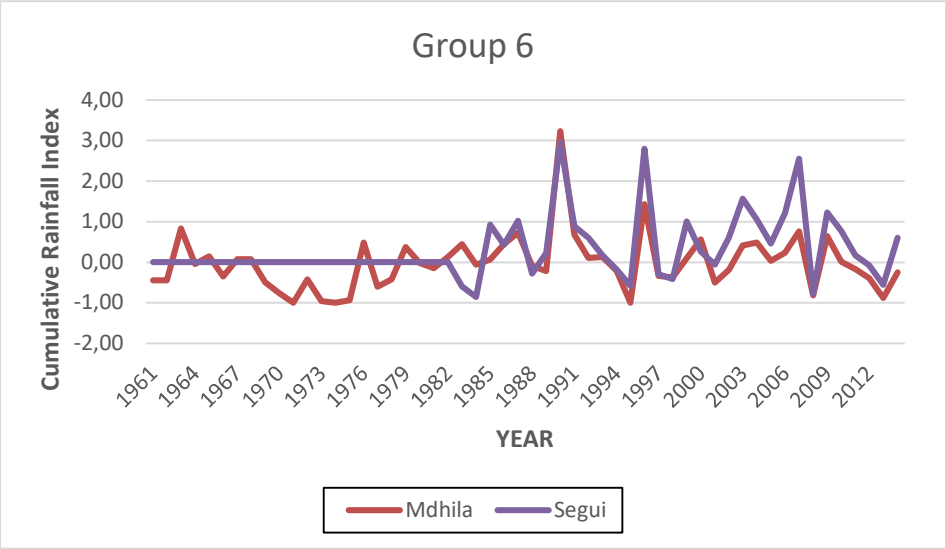

Fig 29 Annual variation of the cumulative rainfall index in group 6

5.4.3. Spatial distribution of rainfall according to the principal component analysis (PCA) and the cumulative rainfall index

The superposition of the results of the study of spatial rainfall variability based on principal component analysis and the cumulative rainfall index divides the basin into five regions (Fig 30).

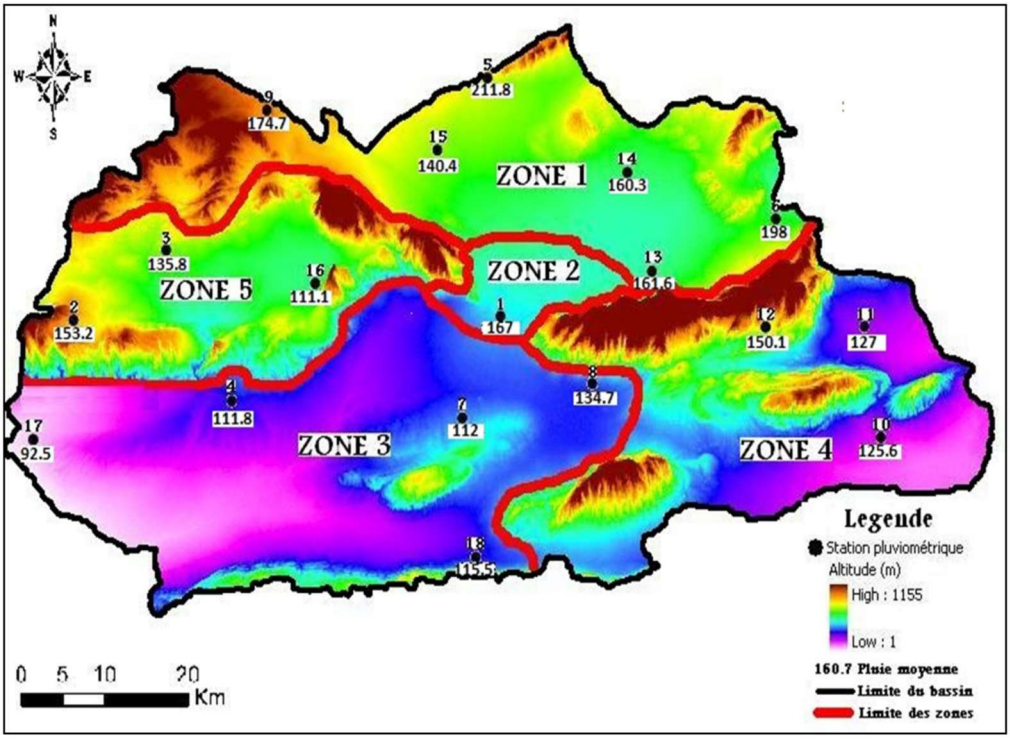

Fig 30 Subdivision of the basin into homogeneous zones based on the cumulative rainfall index (Melki and Abida, 2014).

Each region is characterized by a temporal variation in precipitation and specific physiographic characteristics. The boundaries between the delimited regions have been drawn in consideration of hypsometric characteristics (altitudes) and the spatial distribution of precipitation (isohyets).

Region 1 located in the north of the basin, is characterized by altitudes above 500m. Rainfall records show that this region is the wettest in the study basin.

Region 2 is located in the middle of the basin and corresponds to the transition zone between the first and third regions. The location of this region is affected by all the climatic disturbances that have occurred in the region.

The third region is located in the southern part of the basin, which is characterized by its geographical extension and a hypsometric dominance below 250m. This territory is separated from the northern part by mountainous series and is characterized by low rainfall compared to other regions. The low yield of rainfall in the third zone can be linked to the sensitivity of this zone to Saharan disturbances.

The fourth region is located in the south-eastern part of the basin. This area is identified by the presence of mountain ranges and by average rainfall.

Finally, **the fifth region**, located in the north-western part of the basin, is considered as a closed zone because of its mountainous contour at altitudes above 500m and therefore, it is mainly affected by western climatic disturbances.

The study of the spatial distribution of precipitation shows that the northern region is more humid than the southern area. These regions are separated by mountain ranges (fig 30). It can be deduced, then, that the mountain ranges essentially affect the basin division and the spatial distribution of rainfall.

To conclude, the altitude is a major factor in spatial rainfall distribution, but the existence of some stations with low rainfall despite their high altitudes (station 3 and 12) allows us to deduce that altitude is a main factor in the spatial variability of rainfall, but not the only component.

5.5. Spectral analysis

Spectral analysis is used primarily for the purpose of a general characterisation of the spectral content of each hydrological signal studied. The correlation and spectral analyses correspond to the study of the correlogram and the energy spectrum. The correlogram is calculated by the correlation of the signal with itself, and the energy spectrum is calculated by the Fourier transform of the correlogram. The correlatory and spectral analyses therefore consist in understanding and characterising the behaviour of the system by two different representations of the same information, respectively in the time domain and in the frequency domain (Marsaud, 1997).

5.5.1. Continuous wavelet analysis

Unlike commonly used spectral methods, such as the Fourier transform, the wavelet transform allows a temporal localization of the variability of a given signal. However, hydrological or climatic variability is not expressed in the form of cycles or periods. Wavelets are short oscillating functions that are well localised in time and frequency, with finite energy and zero mean (qualifying condition).According to (Torrence and Compo, 1998); (Perrier et al, 2007); (Mesquita, 2009), the wavelet is a function containing a time parameter (b) and a shape parameter (a). The first allows the wavelet to be stretched for the analysis of the desired frequencies while the second allows the wavelet to be translated on the time axis to analyse the frequency close to a given moment of the signal: function of the wavelet:

$$\psi a, b(t) = \frac{1}{\sqrt{a}} \psi(\frac{t-b}{a})$$

The wavelet chosen for reference is called the mother wavelet and the modification of its parameters produces daughter wavelets. The wavelet transform is therefore performed by decomposing the signal into signals defined over a certain period of time (or space), thus making it possible to analyse variations in frequency content over time. The wavelet transform of a signal s (t) is defined by:

$$s(a,b) = \int_{-\infty}^{+\infty} s(t) \frac{1}{\sqrt{a}} \psi\left(\frac{t-b}{a}\right). dt$$

In this study, the continuous wavelet transform (CWT) was used to obtain reasonably accurate results for both low and high frequencies. Three types of mother wavelets are available in the literature, namely Morlet, Gaussian and Paul wavelets. However, the Morlet mother wavelet was adopted in this study because it has been shown to be more appropriate for the study of rainfall variability (Torrence and Compo, 1998; Perrier et al., 2007, among others). The Morlet wavelet consists of a Gaussian modulated sinus (mathematical function), which essentially has a fairly high frequency resolution. The number of waves in the mother wavelet controls its basic frequency resolution: the higher the number of waves, the faster the wavelet oscillation and the higher the frequency resolution. In particular, applications of discharge wavelet series allow the description of climate oscillation signals (Massei et al., 2009; Massei et al. 2011; Labat et al., 2000, Lafrenieresa and Sharp, 2003).

The continuous wavelet method (WCT) is used to analyse and quantify each temporal feature of the main spectral components of the time series. The wavelet transform is used to track the process at different signal scales (Daubechies, 1990; Zamrane et al., 2016). Several applications of wavelet analysis are possible: isolation of intermittent temporal processes or pumping, characterisation of systems according to their development, study of the temporal structure of floods, etc. (Labat et al. 1999). The main interest of wavelet analysis is to allow a time-scale analysis. Indeed, the wavelet spectrum of the signal allows visualising the presence of temporally localised characteristic frequencies. It thus appears that wavelet analysis is an alternative method to conventional correlative and spectral analysis and is more informative (Labat, 2008).

5.5.2. Identification of the main modes of rainfall variability

According to Torrence and Compo (1998), Perrier et al.,(2007), and Mesquita (2009), the wavelet is a function containing a temporal parameter and a shape parameter. The first allows to stretch the wavelet for the analysis of the desired frequencies while the second allows to translate the wavelet on the times axis to analyse this frequency close to a given moment of the signal.

Continuous wavelet analysis is used to assess and characterise the changing modes of variability in precipitation data series over a short and long term in the catchment GAFSA. The chronicles we have are relatively long, so we can observe the changes in the structure of the

signals. It is also possible to visually compare the spectra of the input and output signals, and to detect possible temporal breaks in the structuring of the rainfall variability. The temporal variability can be expressed as "energy peaks" or "energy bands", covering certain time scales. The local wavelet spectrum allows a description and visualisation of the power distribution (z-axis), from low power values (dark blue) to high power values (red) along the different frequencies (y-axis) over time (x-axis).

The spectra of wavelet analyses of precipitation, applied to monthly rainfall over the period (1970-2014), were analysed for the 18 rainfall stations. The results obtained identified three energy bands (1 (years), 2-4 (years), and 4-8 (years)) for the entire catchment. The wavelet analysis confirms the spatial variability in rainfall in the region and it developed important results in the majority of stations.

A continuous wavelet analysis resulted in detecting the modes and origins of precipitation variability. Three energy bands were clearly identified: (1 (year), 2–4 (years), and 4–8 (years)) for the entire watershed. Moreover, the visualization of the power distribution showed that the modes of variability observed are different in their power distributions from one station to another. Indeed, the approach adopted allowed the identification of two groups with the same characteristics of temporal and frequency variations of precipitation. These two groups were defined according to the difference in occurrence of the frequency band for each station.

The first group, which includes six stations, is characterized by the existence of 1-year frequency bands and few 2- to 4-year bands. The second group, formed by ten stations, presents several bands of annual and inter-annual frequencies (2–4 and 4–8 years). The third group, none of the various modes of variability were developed, it put into consideration that the combination of high altitude and the important values of precipitation reached in the concerned station (station 5 and station 8) may disabled the frequencies of wavelet method to analyse the rainfall variability inside.

To better analyse the wavelet results, they should be grouped according to their shape, to have comparable and meaningful results. The results will be classified into 3 groups each group have numbers of station they react identically with the wavelet calculation and illustrate the same shape. (Fig 31 to 34)

Group 1 :

Six stations (GAFSA SM, Ouled Mansour, Haouel El Oued, Ouled Bou Saad, Hay Amaimia and Sned) compose the first group. According to the subdivision based on cumulative rainfall index (Fig 30, Melki and Abida,2014) all the stations of this 1st group are located in the 1st and 5th zones which are characterised by a mountainous physiography faced with the high altitude, as well as an important values of cumulative rainfall indexes.

(Fig 31)The alternation between high and low energy bands, reflect the succession of wet and dry years, between blue and red spots in the power spectrum ensure the variability of rainfall from period to other. The power of this energy showed differences between all records.

For the (1-year) mode, is showed in all the stations of this group, confirmed by the yellow to red colour in the power spectrum important spatial variability showed. The interruption periods (blue and green spots) may be related to the drought periods that occurred in Tunisia between 1980 and 2000, but it still in between theses discontinuities some extreme events with high values corresponding to 1990s in the majority of the station in group 1.

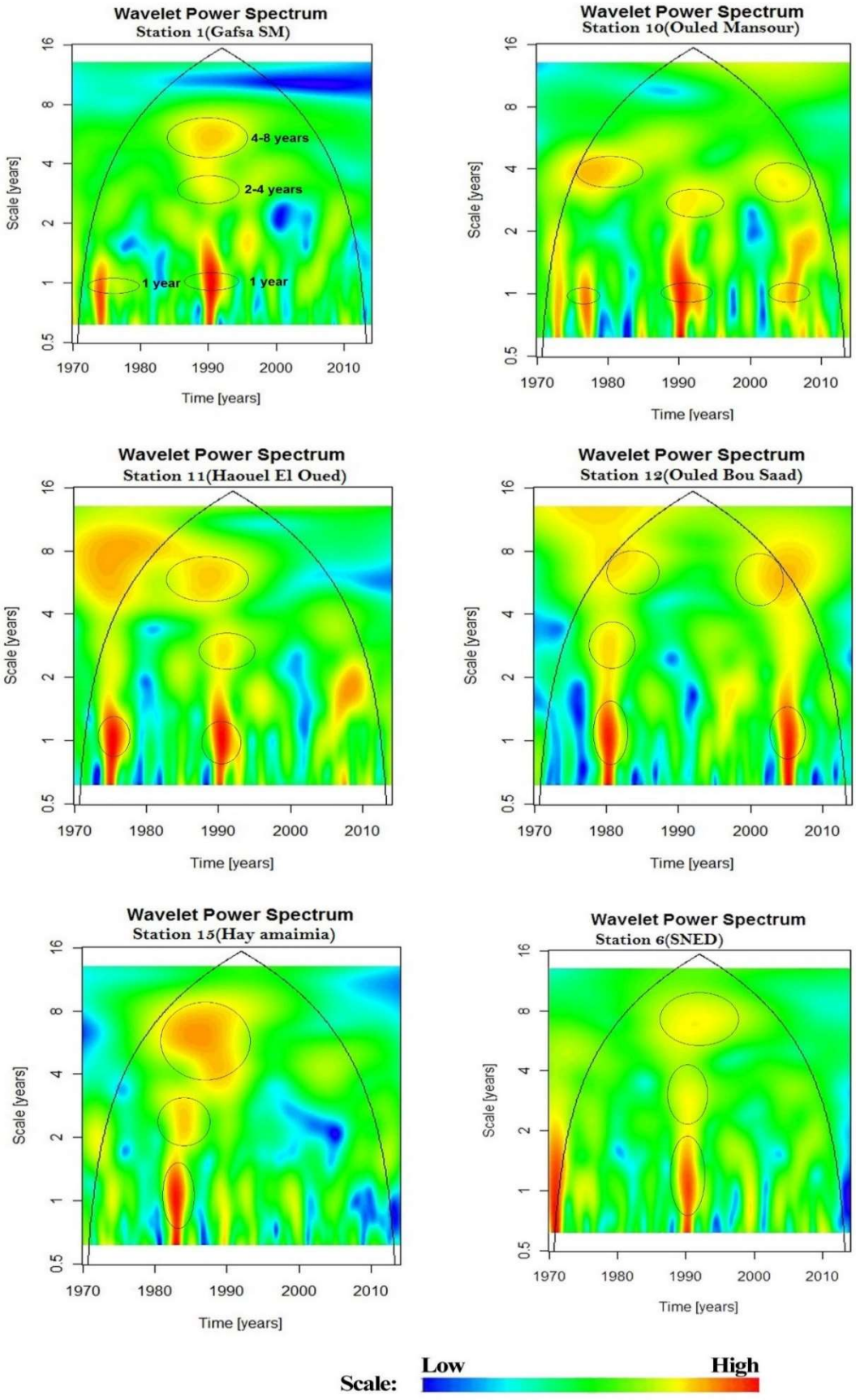

Fig 31 Local spectra of wavelet analysis of monthly rainfall (Group 1)

Group 2:

This group composed by 10 stations in different locations but they does have similar characteristics such as moderated to high altitudes, important values of cumulative rainfall index already confirmed with the (Fig 30) .

The general shape of spectrum power seems to be a sequences of high energy values alternating annually as showing the figure below the yellow to red spots in between bleu zones.

Stations 2, 3, 4 and 7 are reacted similarly in spatial variability identified with an extended red spot during the same period between mid-1980 to early 1990(Fig 32-33).

Frequencies are variable along the period of study, important events were developed identified with the red colour which mean a creation of an important spatial variability inside, also it may due to a global climatic event such as the NAO (North Atlantic Oscillation) because of

the appearance of the two modes of cycles 2-4 and 4-8 years in the 10 stations. These two modes are observed in most stations during the period between (mid 1980s to early 2000s).

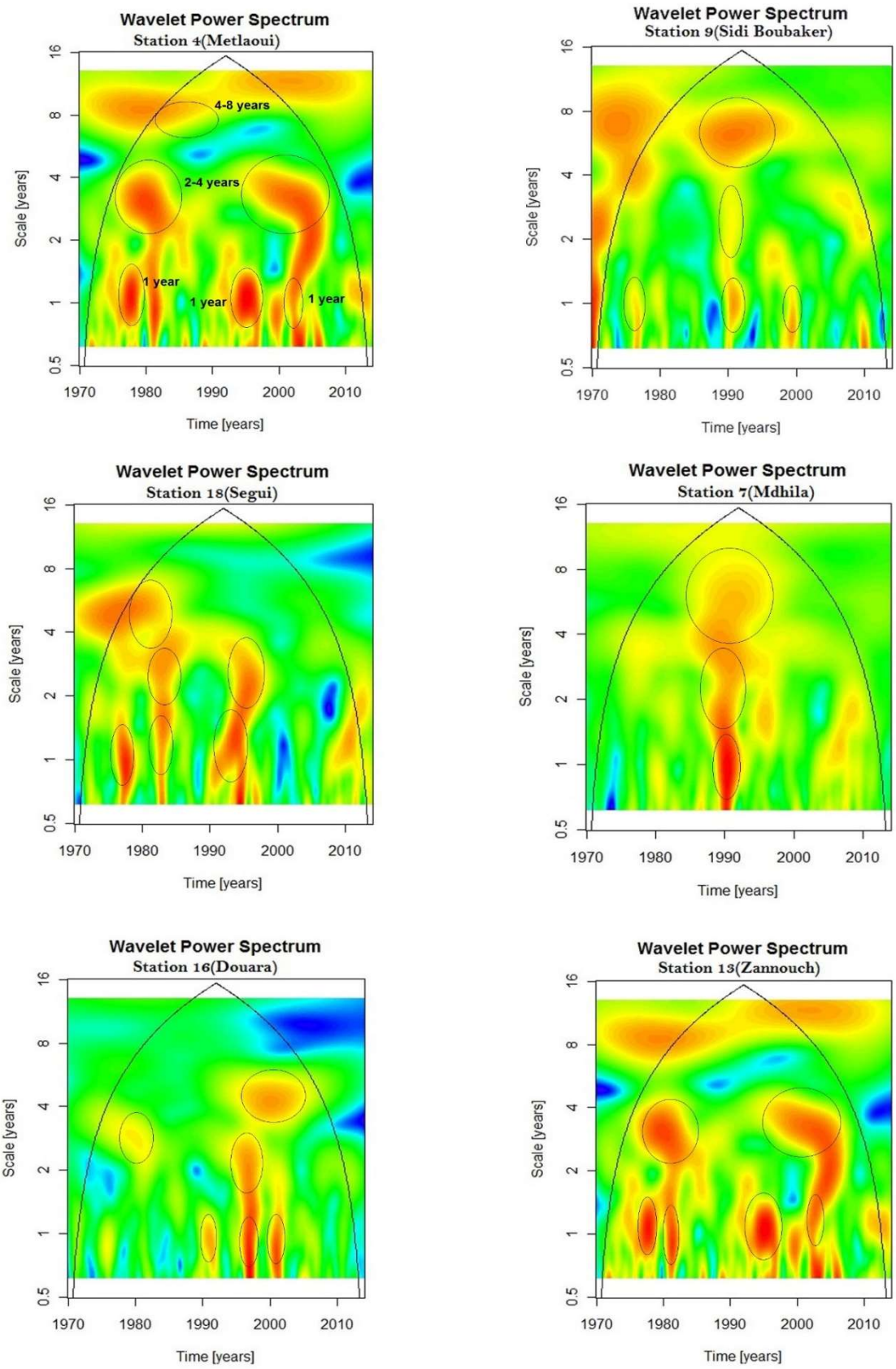

Fig 32 Local spectra of wavelet analysis of monthly rainfall (Group 2)

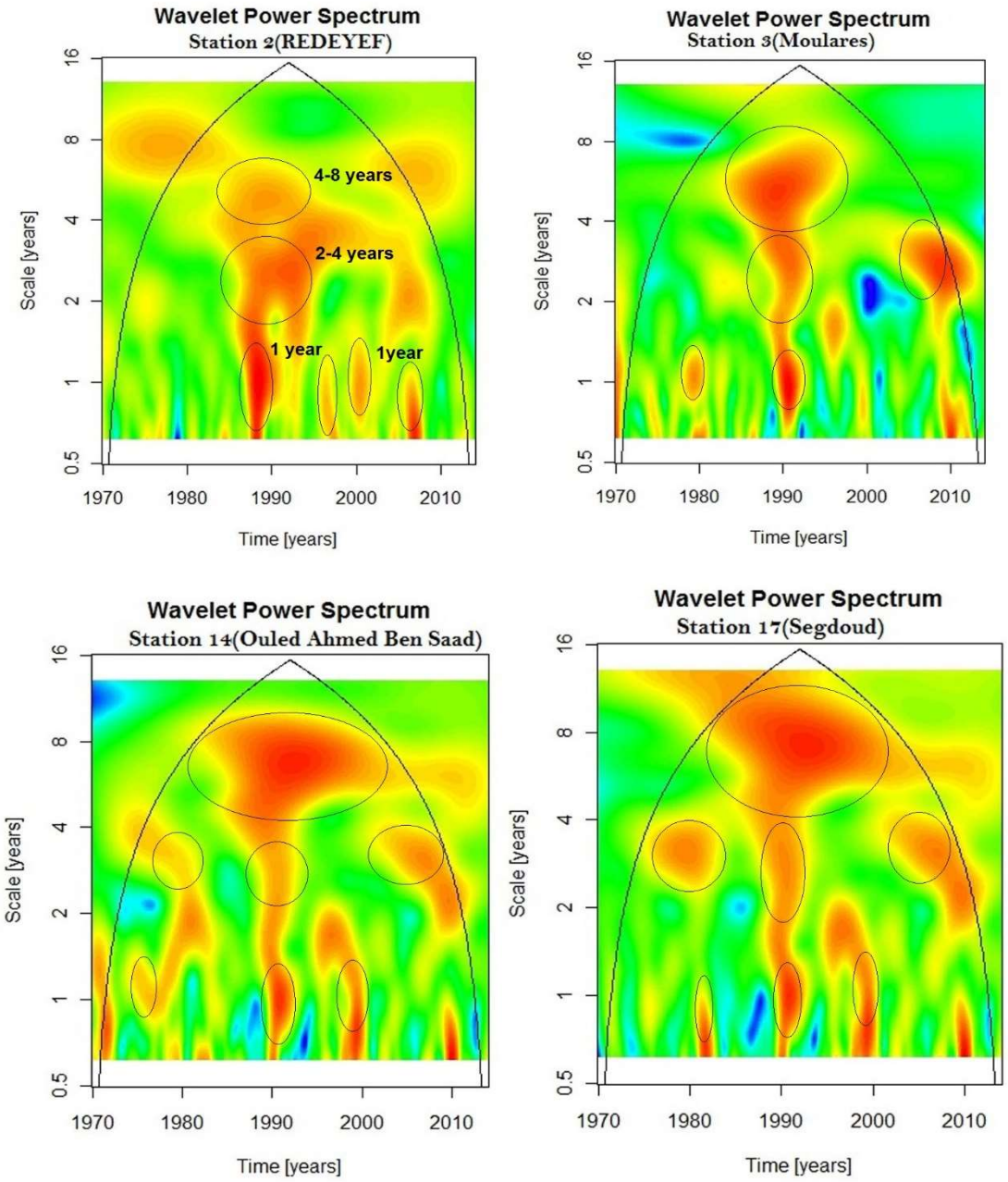

Fig 33 Local spectra of wavelet analysis of monthly rainfall for Group 2(cont.)

Group 3:

Only two stations lefts the 5th and the 8th, no variation during all the period of study, it seems that the wavelet functions are disabled, it may due to the huge variability in rainfall records which is confirmed in the descriptive analysis, these two stations characterised by a succession of blue spots which confirm the low spatial variability unless it recorded some red spots in mid 1970s, it may due again to a global climate phenomena.

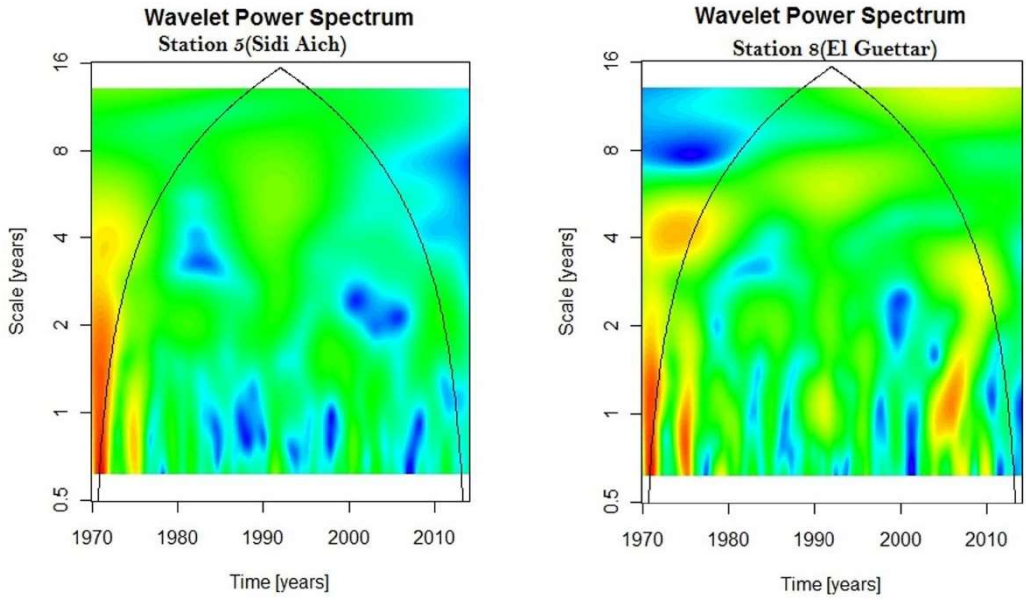

Fig 34 Local spectra of wavelet analysis of monthly rainfall for Group 3

CHAPTER SIX

GENERAL CONCLUSIONS AND RECOMMENDATIONS

6.1 CONCLUSIONS

This study, interested in the analysis of both spatial and temporal variations of rainfall in the Gafsa Basin, based on rainfall data recorded during 56 years (1960-2015) in 18 rainfall stations, resulted in the following conclusions:

The study start with using statistical tools and functions such as HYFRAN in order to fit the evaluation and adaptation of the data sets. It compile a set of tests and distributions; all the rainfall data are independent, stationary and homogenous.

Following by analytical descriptive analysis showed that; rainfall variability in the GAFSA basin is influenced by the effect of topography in the north-eastern regions, while in the south-western regions other factors such as latitude, longitude, proximity to mountains and wind speed direction affect the characteristic precipitation and are the main sources of variation.

The mountain ranges, located in the vicinity of the study basin, act as a climatological barrier and consequently rainfall decreases from north to south and from east to west. Several factors contribute to the spatial variation of rainfall, the most important being altitude, Longitude and latitude also have significant effects on precipitation variability. Statistical indices (number of standard deviations, distribution and frequency) proved that the study watershed is characterised by a very irregular rainfall pattern.

6.2 RECOMMENDATIONS

A continuous wavelet analysis, used to detect the modes and origins of rainfall variability, resulted in the identification of three groups of energies: (1 (year), 2-4 (year) and 4-8 (year)) for the whole watershed. The modes of cycles 2–4 and 4–8 years are two modes that reflect the influence of global climate. Results are ranged according to geographical sitting, morphological characteristics (Altitude and longitude), as well as cumulative rainfall index, all these characteristics enable the wavelet frequencies to manipulate and calculate the spatial irregularity as a tool to evaluate variability in rainfall.

In order to determine and quantify the origin of the differences between the observed modes of precipitation in the GAFSA Watershed, a verification of the coherence between the spatial and temporal variability of precipitation and the climate change models is recommended.

REFERENCES

- Aryal, Y. N. *et al.* (2018) 'Long term Changes in Flooding and Heavy Rainfall Associated with North Atlantic Tropical Cyclones : Roles of the North Atlantic Oscillation and El Niño-Southern Oscillation', *Journal of Hydrology*. doi: 10.1016/j.jhydrol.2018.02.072.
- Baldassarre, G. Di *et al.* (2017) 'Drought and flood in the Anthropocene : feedback mechanisms in reservoir operation', pp. 225–233. doi: 10.5194/esd-8-225-2017.
- Belloumi, M. and Matoussi, S. (2008) 'Local / Global Encounters Water Scarcity Management in the MENA Region from a Globalization Perspective', pp. 135–138. doi: 10.1057/palgrave.development.1100449.
- Benoit, L. *et al.* (no date) 'NORTH ATLANTIC OSCILLATION AND RAINFALL VARIABILITY ON THE SOUTHERN COAST OF THE MEDITERRANEAN', pp. 203–210.
- Buttafuoco, G., Caloiero, T. and Coscarelli, R. (2014) 'Analyses of Drought Events in Calabria (Southern Italy) Using Standardized Precipitation Index'. doi: 10.1007/s11269-014-0842-5.
- Conditions, C. and Pattern, A. (2020) 'G LOBAL P ATTERNS : A RCTIC & N ORTH A TLANTIC O SCILLATIONS', pp. 1–5.
- Debret, M. *et al.* (2009) 'Evidence from wavelet analysis for a mid-Holocene transition in global climate forcing', *Quaternary Science Reviews*. Elsevier Ltd, 28(25–26), pp. 2675–2688. doi: 10.1016/j.quascirev.2009.06.005.
- Di, A. C. G. and Bonaccorso, M. B. (2007) 'Drought forecasting using the Standardized Precipitation Index', pp. 801–819. doi: 10.1007/s11269-006-9062-y.
- Dr.*Achraf MELKI*, G. D. E., Sciences, E. N. and Terre, D. E. L. A. (2017).
- Du, J. *et al.* (2013) 'Analysis of dry / wet conditions using the standardized precipitation index and its potential usefulness for drought / flood monitoring in Hunan Province , China', pp. 377–387. doi: 10.1007/s00477-012-0589-6.
- Dutra, E. *et al.* (2013) 'Seasonal forecasts of droughts in African basins using the Standardized Precipitation Index', pp. 2359–2373. doi: 10.5194/hess-17-2359-2013.
- Ellouze, M., Azri, C. and Abida, H. (2009) 'Spatial variability of monthly and annual rainfall data over Southern Tunisia', *Atmospheric Research*. Elsevier B.V., 93(4), pp. 832–839. doi: 10.1016/j.atmosres.2009.04.005.
- Ersion, V., Adlouni, S. El and Bobée, B. (2015) 'Professeur , Département de

Mathématiques et de statistique , Université de Moncton Professeur Émérite Version of the 13 th of January 2015 Note : Documents listed in the references (page 61) and marked by * are available when installing the DEMO version of the software Citation : El Adlouni , S . and B . Bobée (2015). Hydrological Frequency Analysis Using Software . User ' s Guide available with the software DEMO http://www.wrpllc.com/books/HyfranPlus/indexhyfranplus3.html', (1), pp. 1–71.

- Gergis, J. L. and Fowler, A. M. (2009) *A history of ENSO events since A . D . 1525 : implications for future climate change*. doi: 10.1007/s10584-008-9476-z.
- Gleick, P. H. (1999) 'The human right to water', 1(1998), pp. 487–503.
- Heinemann, A. B. *et al.* (no date) 'This article is protected by copyright. All rights reserved.' doi: 10.1002/joc.6684.
- Hurrell, J. W. *et al.* (2018) *North Atlantic Oscillation (NAO) ☆*. 3rd edn, *Encyclopedia of Ocean Sciences, 3rd Edition*. 3rd edn. Elsevier Inc. doi: 10.1016/B978-0-12-409548-9.11621-5.
- Is, W. and Component, P. (2020) 'A step by step explanation of principal component analysis'.
- Jemai, H, Manel Ellouze, Habib Abida and Benoit Laignel (2018) 'Spatial and temporal variability of rainfall : case of Bizerte-Ichkeul Basin'. Arabian Journal of Geosciences.
- Jemai, S., Kallel, A. and Abida, H. (2018) 'Drought distribution using the standardized precipitation index : case of Gabes Basin , South Tunisia'. Arabian Journal of Geosciences.
- Jr, R. A. P. and Landsea, C. N. (1999) 'and Atlantic Hurricane Damages in the United States', (1994), pp. 2027–2033.
- Keefer, D. K., Moseley, M. E. and Susan, D. (2003) 'A 38 000-year record of £ oods and debris £ ows in the Ilo region of southern Peru and its relation to El Nin ‹ o events and great earthquakes', 194. doi: 10.1016/S0031-0182(03)00271-2.
- Livada, I. and Assimakopoulos, V. D. (2007) 'Spatial and temporal analysis of drought in Greece using the Standardized Precipitation Index (SPI)', 153, pp. 143–153. doi: 10.1007/s00704-005-0227-z.
- López-moreno, J. I. *et al.* (2011) 'Effects of the North Atlantic Oscillation (NAO) on combined temperature and precipitation winter modes in the Mediterranean mountains : Observed relationships and projections for the 21st century', *Global and*

Planetary Change. Elsevier B.V., 77(1–2), pp. 62–76. doi: 10.1016/j.gloplacha.2011.03.003.

- Michiels, E., Gabriels, D. and Hartmann, R. (1992) 'Using the Seasonal and Temporal Precipitation Concentration Index for Characterizing the Monthly Rainfall Distribution in Spain', 19, pp. 43–58.
- Ortlleb, L. (1993) 'Former E1 Nifio events : records from western South America', 7, pp. 181–202.
- Ruy, J. *et al.* (2014) 'Annual maximum daily rainfall trends in the Midwest , southeast and southern Brazil in the last 71 years', *Weather and Climate Extremes*. Elsevier, 5–6, pp. 7–15. doi: 10.1016/j.wace.2014.10.001.
- Sigdel, M. and Ikeda, M. (2010) 'Spatial and Temporal Analysis of Drought in Nepal using Standardized Precipitation Index and its Relationship with Climate Indices', (December), pp. 59–74.
- Vairavamoorthy, K., Gorantiwar, S. D. and Pathirana, A. (2008) 'Managing urban water supplies in developing countries – Climate change and water scarcity scenarios', 33, pp. 330–339. doi: 10.1016/j.pce.2008.02.008.
- Visbeck, M. H. *et al.* (2000) 'From the Academy The North Atlantic Oscillation : Past , present , and future', pp. 2000–2001.
- Wu, H. *et al.* (2007) 'Appropriate application of the Standardized Precipitation Index in arid locations and dry seasons', 79(June 2006), pp. 65–79. doi: 10.1002/joc.